bioRxiv preprint doi: https://doi.org/10.1101/2025.01.15.633108; this version posted January 15, 2025. The copyright holder for this preprint (which was not certified by peer review) is the author/funder. All rights reserved. No reuse allowed without permission.

Neurite density but not myelination of specific fiber tracts links polygenic scores to general intelligence

Christina Stammen[a], Javier Schneider Penate[b], Dorothea Metzen[c], Maurice J. Hönscher[d], Christoph Fraenz[a], Caroline Schlüter[d], Onur Güntürkün[d,e], Robert Kumsta[e,f,g], Erhan Genç[a]*

[a]: Department of Psychology and Neuroscience, Leibniz Research Centre for Working Environment and Human Factors (IfADo), 44139 Dortmund, Germany

[b]: Department of Neuropsychology, Institute of Cognitive Neuroscience, Faculty of Psychology, Ruhr University Bochum, 44801 Bochum, Germany

[c]: Institute of Psychology, Department of Educational Sciences and Psychology, TU Dortmund University, 44227 Dortmund, Germany

[d]: Biopsychology, Institute for Cognitive Neuroscience, Faculty of Psychology, Ruhr University Bochum, 44801 Bochum, Germany

[e]: German Center for Mental Health (DZPG), partner site Bochum/Marburg, Germany

[f]: Genetic Psychology, Faculty of Psychology, Ruhr University Bochum, Bochum, Germany

[g]: Department of Behavioural and Cognitive Sciences, Laboratory for Stress and Gene-Environment Interplay, University of Luxemburg, Luxemburg

*: Corresponding author: Prof. Dr. Erhan Genç; Telephone: +49 231 1084520; Email: genc@ifado.de; Address: Department of Psychology and Neuroscience, Leibniz Research Centre for Working Environment and Human Factors (IfADo), Ardeystraße 67, 44139 Dortmund, Germany.

ORCID IDs: Dorothea Metzen: 0000-0002-4250-0076; Caroline Schlüter: 0000-0003-3684-3096; Onur Güntürkün: 0000-0003-4173-5233; Robert Kumsta: 0000-0001-6006-6958; Erhan Genç: 0000-0001-6514-5479

bioRxiv preprint doi: https://doi.org/10.1101/2025.01.15.633108; this version posted January 15, 2025. The copyright holder for this preprint (which was not certified by peer review) is the author/funder. All rights reserved. No reuse allowed without permission.

Abstract

White matter is fundamental for efficient and accurate information transfer throughout the human brain and thus crucial for intelligence. Previous studies often demonstrated associations between fractional anisotropy (FA) as a metric of white matter "microstructural integrity" and intelligence, but it is still unclear, whether this relation is due to greater axon density, parallel, homogenous fiber orientation distributions, or greater myelination since all of these measures influence FA. Using neurite orientation dispersion and density imaging (NODDI) and myelin water fraction (MWF) imaging data, we analyzed the microstructural architecture of intelligence in more detail in a sample of 500 healthy young adults. Furthermore, we were interested whether specific white matter microstructural indices play intermediary roles in the pathway that links genetic disposition for intelligence to phenotype. Thus, we conducted for the first time mediation analyses investigating whether neurite density (NDI), orientation dispersion (ODI), and MWF of 64 white matter fiber tracts mediate the effects of polygenic scores for intelligence (PGS_{GI}) on general intelligence. By doing so, we showed that NDI, but not ODI or MWF of white matter fiber tracts was significantly associated with general intelligence and that the NDI of six fiber tracts mediated the relation between genetic variability and *g*. These findings are a crucial step forward in decoding the neurogenetic underpinnings of general intelligence, as they identify that neurite density of specific fiber tracts relates polygenic variation to *g*, whereas orientation dispersion and myelination did not.

Keywords: general intelligence, myelin water fraction, neurite density, orientation dispersion, polygenic scores

bioRxiv preprint doi: https://doi.org/10.1101/2025.01.15.633108; this version posted January 15, 2025. The copyright holder for this preprint (which was not certified by peer review) is the author/funder. All rights reserved. No reuse allowed without permission.

Introduction

Intelligence usually refers to the "[…] ability to understand complex ideas, to adapt effectively to the environment, to learn from experience, to engage in various forms of reasoning, to overcome obstacles by taking thought" [1]. It is one of the most studied human phenotypes and the last decades have produced cognitive tests in abundance to measure intelligence [2]. Although the various tests capture different aspects of intelligence, such as reasoning abilities or processing speed [3], individuals who perform well on one test tend to achieve high scores on other cognitive tests, regardless of the skills required [4,2]. Spearman [4] concluded that there was a factor of general intelligence, *g*, positioned at the apex of the hierarchy, with broader cognitive domains situated below and more specific cognitive abilities at the base [3,5]. The *g* factor illustrates the generalist character of intelligence [6], which is also reflected in the numerous associated life outcomes, such as school performance [7], job performance [8], socioeconomic success [9], income [10], or physical health [11]. In addition to the predictive value of intelligence, interindividual differences have been shown to be stable across the lifespan [12]. Consequently, there have been countless research efforts to uncover the neurogenetic mechanisms from which interindividual differences in intelligence arise.

A well-known framework for understanding intelligence on a neurobiological level provides the Parieto-Frontal Integration Theory of intelligence (P-FIT) [13]. This model suggests that intelligence is based on numerous areas throughout the cortex, especially in frontal and parietal regions, which are strongly interconnected and enable efficient information transfer. The idea that a brain network underlies intelligence also emphasized the role of structural connections, which are present in the form of white matter fiber tracts [13].

One technique to quantify white matter properties is diffusion-weighted imaging (DWI), whose advent has ushered in a new era of white matter brain imaging studies [2,14]. As the diffusion of water molecules is a three-dimensional process that includes random translational motion of molecules in space, diffusion anisotropy allows inferences about the presence of obstacles such as axons and their myelin sheaths [14]. Most studies use fractional anisotropy (FA) as a summative metric to describe white matter microstructural integrity [15]. In this context, higher FA values suggest more parallel diffusion pathways [16,17].

The relation between FA and intelligence has been widely studied [18-35]. The majority of studies reported positive associations between average FA values from many major white matter fiber tracts and cognitive performance [15]. Cox et al. [26], for example, used a large sample from the UK Biobank study and reported significant positive associations between FA and general intelligence in 25 out of 27 white matter fiber tracts. As summarized by Genç, Fraenz [15], FA values of the genu and the splenium of the corpus callosum, the uncinate fasciculus, and the superior longitudinal fasciculus were most often associated with differences

bioRxiv preprint doi: https://doi.org/10.1101/2025.01.15.633108; this version posted January 15, 2025. The copyright holder for this preprint (which was not certified by peer review) is the author/funder. All rights reserved. No reuse allowed without permission.

in intelligence. In one recent study, Stammen et al. [34] showed robust associations between FA and general intelligence in four independent samples, located around the left-hemispheric forceps minor, superior longitudinal fasciculus, and cingulum-cingulate gyrus.

Since general intelligence appears to be robustly associated with higher FA values and thus stronger anisotropic diffusion patterns, Stammen et al. [34] formulated three possible explanations as to why higher FA values could be associated with higher intelligence. First, the relation could be due to greater axon density, enabling more parallel information processing by providing more pathways to think through problems relatively simultaneously. Second, the relation could be due to parallel, homogenous fiber orientation distributions that run directly from one brain region to another, thereby enabling more direct and efficient information transfer throughout the brain. Third, the relation could be due to greater myelination, enabling faster information processing speed and signal conduction velocity [36,37]. However, the exact neurobiological basis causing FA signal differences remains unclear, so the hypotheses put forward cannot be tested by looking at FA values alone. FA is a multifaceted and non-specific metric influenced by various physiological factors, including axon diameter, fiber density, myelin concentration, or the distribution of fiber orientation [38,14,39,40].

Recent advances in neuroimaging offer promising techniques that allow more differentiated and specific conclusions to be drawn about the microstructure of white matter and the three hypotheses mentioned [40]. Neurite orientation dispersion and density imaging (NODDI) [41] and myelin water fraction (MWF) imaging [42,37] both are non-invasive, but take advantage of the unique patterns that water molecules create in different environments.

NODDI utilizes a three-compartment model that differentiates between intra-neurite, extra-neurite, and cerebrospinal fluid (CSF) environments based on a multi-shell high-angular-resolution diffusion imaging protocol [41]. While isotropic diffusion occurs mainly in regions with CSF, intracellular compartments are characterized by stick-like or cylindrically symmetrical diffusion, as the water molecules are restricted by the membranes of neurites, and extracellular compartments by hindered diffusion, as there are many cellular membranes of somas and glia cells. The different diffusion properties allow the estimation of NODDI markers as approximations for different aspects of neurite morphology, such as the neurite density index (NDI), which represents the volume fraction of intra-neurite environments, and the orientation dispersion index (ODI), which quantifies the angular variation of neurite dispersion [41]. Histological studies supported the validity of the NODDI model [43].

MWF imaging relies on signals from myelin water, as signals from larger molecules such as lipids and proteins (main components of myelin) quickly decay to zero [42,37]. Unmyelinated neurons and glia cells have single bilayer membranes, whereas myelinated neurons possess multi-bilayer membranes, with roughly 40% of their mass consisting of compartmentalized

bioRxiv preprint doi: https://doi.org/10.1101/2025.01.15.633108; this version posted January 15, 2025. The copyright holder for this preprint (which was not certified by peer review) is the author/funder. All rights reserved. No reuse allowed without permission.

water [42]. Although there is currently no method capable to measure the myelin bilayer directly, MWF imaging is considered the method of choice to estimate myelin content *in vivo* [42,37]. Studies validated the specificity of MWF imaging mapping the myelin bilayer by comparison with histological results [44-47] and demonstrated that MWF imaging has good reliability [48-51].

Thus, the question of whether the association between higher FA values and higher intelligence is due to greater axon density, parallel, homogenous fiber orientation distributions, or greater myelination can be answered by associating general intelligence with the corresponding indices NDI, ODI, and MWF. However, there are few to no studies that have used NODDI or MWF imaging in relation to intelligence.

Regarding NODDI, Genç et al. [52] were the first to analyze the microstructural architecture of intelligence. They showed that higher intelligence was associated with lower NDI and ODI in the gray matter and thus concluded that the neuronal circuitry linked to higher intelligence is structured in a sparse and efficient way [52]. For white matter, which is more relevant for this paper, associations between NODDI metrics and individual cognitive functions such as paired associate learning [53], episodic memory [54], or processing speed [54] have been reported in healthy adults. Callow et al. [55] found that the ODI of the cerebellar peduncle was significantly associated with fluid, but not crystallized cognition in healthy young adults.

To the best of our knowledge, there is no paper to date that analyzed MWF with regard to general intelligence in healthy adults. Penke et al. [20] were the first to use a biomarker of myelin, magnetization transfer ratio (MTR), to study intelligence in a sample of healthy older people. They were able to show that MTR correlated significantly with general intelligence. However, although a change in myelin content causes a change in MTR, MTR is also influenced by other pathological factors [42,56,57], so MTR is not as specific to myelin as MWF [42,37]. The relation between MWF and cognitive abilities in healthy adults has only been studied for specific cognitive functions such as processing speed [58], executive functions [59], or memory performance [60], but not for general intelligence.

To better understand the microstructural architecture of general intelligence, our study aimed to analyze the relation between general intelligence and NDI, ODI, and MWF within the same sample, with all indices extracted from the same 64 white matter fiber tracts. To further complete the picture, we did not limit our analyses to the relation between the brain and intelligence, but included genes and directly considered the triad between genes, the brain, and behavior via mediation analyses.

General intelligence is a highly heritable trait, with inherited differences in desoxyribonucleic acid (DNA) sequence explaining for about half of the variance in intelligence across all ages [61,6,62,2]. However, heritability of intelligence is not due to few individual genes, but results

bioRxiv preprint doi: https://doi.org/10.1101/2025.01.15.633108; this version posted January 15, 2025. The copyright holder for this preprint (which was not certified by peer review) is the author/funder. All rights reserved. No reuse allowed without permission.

from thousands of genetic variants, mostly single nucleotide polymorphisms (SNPs), whose small effects on the variation of intelligence add up [2,6]. Polygenic scores (PGS) offer the possibility to account for this highly polygenic architecture by aggregating the effects of different SNPs across the genome into a summarized measure [63]. Results of genome-wide association studies (GWAS), used to identify which SNPs throughout the genome are statistically associated with a particular trait, show which of the two alleles for a SNP is positively associated with the trait (called increasing allele) and provide effect sizes for each SNP [2,6]. A PGS is constructed by summing the number of increasing alleles associated with intelligence across SNPs and weighting them by the respective effect size obtained from GWAS [2,6]. PGS for intelligence, derived from one of the largest GWAS to date based on 269,867 individuals, explain up to 5.2% of variance in general intelligence in independent samples [64].

Genetic correlations show that the genetic variants associated with intelligence are partially consistent with those associated with brain structure [2,65]. White matter microstructure has been shown to be highly polygenic as well and positive genetic correlations with higher intelligence have been identified [2,66-68]. The gene sets significantly associated with intelligence include neurogenesis, neuron differentiation, central nervous system neuron differentiation, regulation of nervous system development, positive regulation of nervous system development, and regulation of synapse structure or activity [64]. While other GWAS analyses on intelligence reported similar gene sets [65,69], gene sets such as myelin sheath or regulation of myelination were not found to be significantly related to intelligence in any study. Lee et al. [70], who performed a large GWAS on educational attainment, also found no gene sets related to glial cells that were positively enriched and concluded that differences in cognition may not necessarily be driven by differences in myelination and thus transmission speed.

Mediation analyses blaze the best trail to investigate the relation between PGS for general intelligence (PGS_{GI}), microstructural white matter indices (NDI, ODI, and MWF), and general intelligence. However, there are only few mediation studies in healthy adults investigating the relation between genes, the brain, and intelligence and those that exist have focused their analyses on mediation effects of total brain volume, surface area, cortical thickness, white matter fiber network efficiency, and functional efficiency [71-75]. Although Genç et al. [72] found the white matter fiber network efficiency of two brain areas to be mediators regarding the effects of PGS on general intelligence using data from the same sample, they did not include white matter microstructure indices in their analyses, and to the best of our knowledge, other studies have not used such indices in mediation analyses in healthy adults either.

To summarize, NODDI and MWF imaging, with their indices NDI, ODI, and MWF, offer opportunities to analyze the microstructural architecture of intelligence on a new level and draw

bioRxiv preprint doi: https://doi.org/10.1101/2025.01.15.633108; this version posted January 15, 2025. The copyright holder for this preprint (which was not certified by peer review) is the author/funder. All rights reserved. No reuse allowed without permission.

more differentiated and specific conclusions regarding the question whether the association between higher FA values and higher intelligence is due to greater axon density (NDI), parallel, homogenous fiber orientation distributions (ODI), or greater myelination (MWF). While these opportunities have only been used selectively for NODDI, to our knowledge there is no study that has investigated the relation between MWF and general intelligence in healthy young adults, so we performed this analysis here for the first time. Furthermore, we expanded the existing literature on mediation analyses regarding the relations between genes, the brain, and intelligence to include white matter microstructure. We analyzed the effects of PGS_{GI} on general intelligence and tested the mediating role of NDI, ODI, and MWF of 64 white matter fiber tracts in a large sample of at least 500 individuals. Thus, this study presents the first mediation analyses that give insight whether white matter microstructure indices provide a biological pathway through which our genetics influence general intelligence.

bioRxiv preprint doi: https://doi.org/10.1101/2025.01.15.633108; this version posted January 15, 2025. The copyright holder for this preprint (which was not certified by peer review) is the author/funder. All rights reserved. No reuse allowed without permission.

Methods

Participants

The sample consisted of 557 adults with a mean age of 27.33 years (SD = 9.43 years; range: 18-75 years, 503 right-handers), including 283 men (mean age = 27.71 years; SD = 9.86 years, 246 right-handers) and 274 women (mean age = 26.94 years; SD = 8.96 years, 257 right-handers). It has previously been used to investigate relations between genetic variability, brain properties, and intelligence [72]. Handedness was assessed using the Edinburgh Handedness Inventory [76]. Participants were mostly university students of different majors (mean years of education = 17.14 years; SD = 3.12 years), who were either financially compensated for their participation or received course credits. Individuals who had insufficient German language skills or reported having done any of the employed intelligence tests within the last five years were excluded from the study. Health status was assessed by a self-report questionnaire. Individuals were also not admitted to the study if they or any of their close relatives suffered currently or in the past from neurological and/or mental illnesses. The study protocol was approved by the Local Ethics Committee of the Faculty of Psychology at Ruhr University Bochum (vote Nr. 165). All participants gave written informed consent and were treated according to the Declaration of Helsinki.

Acquisition and analysis of behavioral data

General intelligence was assessed by the use of four paper-and-pencil tests. The tests were conducted in a quiet and well-lit room.

I-S-T 2000 R

The Intelligenz-Struktur-Test 2000 R (I-S-T 2000 R) [77] is a well-established German intelligence test battery, requiring about 2.5 hours to complete. It evaluates various aspects of intelligence as well as general intelligence and is largely comparable to the internationally established Wechsler Adult Intelligence Scale Forth Edition [78]. The majority of included cognitive test items are presented in multiple-choice format. The test consists of a basic and an extension module. Within the basic module, verbal, numerical, and figural abilities are each assessed by three different mental reasoning tasks of 20 items. Verbal intelligence is assessed by tasks in which participants must complete sentences (IST_SEN), find analogies (IST_ANA), and recognize similarities (IST_SIM). Numerical intelligence is assessed by tasks involving arithmetic calculations (IST_CAL), number series (IST_SER), and mathematical equations to which arithmetic signs need to be added (IST_SIG). Figural intelligence is assessed by tasks in which participants must select and reassemble parts of a cut-up figure (IST_SEL), mentally rotate and match three-dimensional objects (IST_CUB), and solve matrix-reasoning problems (IST_MAT). In addition, retention (IST_RET) is assessed by ten verbal and 13 figural items. Here, participants must memorize series of words or figure pairs. The extension module

bioRxiv preprint doi: https://doi.org/10.1101/2025.01.15.633108; this version posted January 15, 2025. The copyright holder for this preprint (which was not certified by peer review) is the author/funder. All rights reserved. No reuse allowed without permission.

comprises 84 multiple-choice questions on six knowledge facets (art/literature, economy, geography/history, mathematics, science, and daily life) and measures general knowledge (IST_KNO). Reliability estimates (Cronbach's α) are between .88 and .96 for subtests and composite scores. The recent norming sample consists of about 5800 individuals for the basic module and 661 individuals for the extension module. The age range in the norming sample is between 15 and 60 years and both sexes are represented equally [77].

BOMAT-Advanced Short

The Bochumer Matrizentest (BOMAT) [79] is a non-verbal German intelligence test which is widely used in neuroscientific research [79-82,52,83,84] and whose structure resembles that of the well-established Raven's Advanced Progressive Matrices [85]. Within the framework of our study, we employed the advanced short version, which is characterized by high discriminatory power in samples with generally high intellectual abilities, thus avoiding possible ceiling effects [52,83]. The test comprises two parallel forms with 29 matrix-reasoning items. Each item shows a 5-by-3 matrix composed of elements arranged according to a specific but unspecified rule. One field within the matrix is empty and needs to be filled with one of six provided elements that follows the rule. The participants were assigned to one of the two parallel forms and had to complete as many matrices as possible within a time limit of 45 minutes. Split-half reliability of the BOMAT is .89, Cronbach's α is .92, and reliability between the parallel forms is .86. The recent norming sample consists of about 2100 individuals with an age range between 18 and 60 years and equal sex representation [79].

BOWIT

The Bochumer Wissenstest (BOWIT) [86] is a German general knowledge questionnaire. It assesses eleven different knowledge facets, from two major domains. The four facets biology/chemistry, mathematics/physics, nutrition/exercise/health, and technology/electronics are assigned to the scientific-technical knowledge domain. The social and humanistic knowledge domain includes seven facets: arts/architecture, civics/politics, economies/laws, geography/logistics, history/archaeology, language/literature, and philosophy/religion. The BOWIT is available in two parallel test forms, in which each knowledge facet is represented by 14 multiple-choice questions. To measure general knowledge as precisely as possible, all participants had to complete both test forms, resulting in 308 items. The BOWIT shows reliability estimates greater than .90: split-half reliability is reported as .96, Cronbach's α .95, test-retest reliability .96, and parallel-form reliability .91. The recent norming sample consists of about 2300 individuals with an age range between 18 and 66 years and equal sex representation [86].

bioRxiv preprint doi: https://doi.org/10.1101/2025.01.15.633108; this version posted January 15, 2025. The copyright holder for this preprint (which was not certified by peer review) is the author/funder. All rights reserved. No reuse allowed without permission.

ZVT

The Zahlenverbindungstest (ZVT) [87] is a trail-making test used to assess the cognitive processing speed of both children and adults. After completing two short sample tasks, four main tasks are assessed. Here, participants connect numbers from 1 to 90 according to a specific rule as fast as possible. The processing times for the four tasks are averaged to obtain an overall measure of processing speed. The reliability across the four tasks is reported as .95 in adults. The six-month retest-reliability is reported to be between .84 and .90. The recent norming sample consists of about 2109 individuals with an age range between eight and 60 years and equal sex representation [87].

Computation of the general intelligence factor, *g*

We computed the general intelligence factor to provide a comparable and robust measure of intelligence. When included tests measure intelligence broadly enough, *g* factors derived from different test batteries are statistically equivalent [88,89]. As described in Stammen et al. [34], we used the intelligence test scores to compute *g* factor scores for every participant. After regressing age, sex, age*sex, age^2, and age^2*sex from the test scores, we used the standardized residuals to develop a hierarchical factor model via exploratory factor analysis. Subsequently, we performed confirmatory factor analysis to assess model fit using the chi-square (X^2) statistic as well as the fit indices Root Mean Square Error of Approximation (RMSEA), Standardized Root Mean Square Residual (SRMR), Comparative Fit Index (CFI), and Tucker-Lewis Index (TLI). The evaluation of model fit yielded good fit. Although the chi-square (X^2) statistic assessing the magnitude of discrepancy between the model-implied variance-covariance matrix and the empirically observed variance-covariance matrix [90] was significant ($X^2(64) = 127.97$, $p < .001$), this did not itself show poor model fit since the chi-square (X^2) statistic is a direct function of sample size meaning that the probability of rejecting any model increases with greater sample size [91,92]. The other fit indices (RMSEA = .042, SRMR = .033, CFI = .979, and TLI = .969) were all acceptable as values of RMSEA and SRMR less than .05 and values of CFI and TLI greater than .97 are considered good [90]. Based on the postulated confirmatory factor model shown in Figure 1, we calculated regression-based *g*-factor scores for every participant, winsorizing outliers [93].

bioRxiv preprint doi: https://doi.org/10.1101/2025.01.15.633108; this version posted January 15, 2025. The copyright holder for this preprint (which was not certified by peer review) is the author/funder. All rights reserved. No reuse allowed without permission.

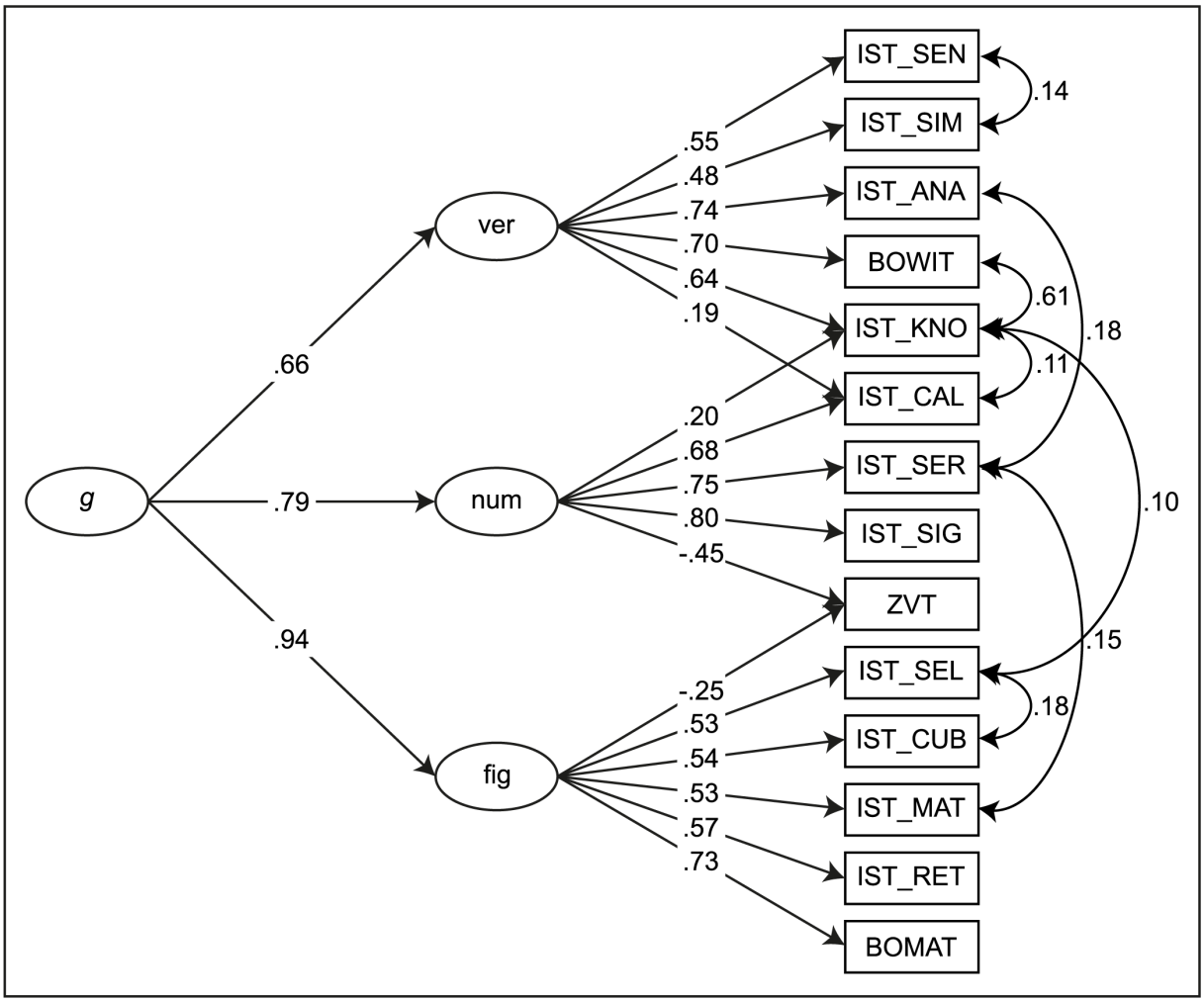

Fig. 1 Confirmatory factor analytic model. *g* = general factor of intelligence, ver = verbal intelligence as broad cognitive domain, num = numerical intelligence as broad cognitive domain, fig = figural intelligence as broad cognitive domain, IST_SEN = subtest Sentence Completion of the I-S-T 2000 R, IST_SIM = subtest Similarities of the I-S-T 2000 R, IST_ANA = subtest Analogies of the I-S-T 2000 R, BOWIT = Bochumer Wissenstest, IST_KNO = parameter Knowledge of the I-S-T 2000 R, IST_CAL = subtest Calculations of the I-S-T 2000 R, IST_SER = subtest Number Series of the I-S-T 2000 R, IST_SIG = subtest Numerical Signs of the I-S-T 2000 R, ZVT = Zahlenverbindungstest, IST_SEL = subtest Figure Selection of the I-S-T 2000 R, IST_CUB = subtest Cubes of the I-S-T 2000 R, IST_MAT = subtest Matrices of the I-S-T 2000 R, IST_RET = parameter Retentiveness of the I-S-T 2000 R, BOMAT = Bochumer Matrizentest

Intelligence level

Unfortunately, it is not possible to link *g* to the intelligence quotient (IQ) scale. Nevertheless, we used norming data of some tests to estimate the intelligence level. Norming data of the subtests of the I-S-T 2000 R revealed that the sample's mean IQ was 115 (SD = 13.0). The fact that our sample had a mean score one standard deviation above average may have impacted the associations with the polygenic scores and the white matter fiber tracts' microstructure.

bioRxiv preprint doi: https://doi.org/10.1101/2025.01.15.633108; this version posted January 15, 2025. The copyright holder for this preprint (which was not certified by peer review) is the author/funder. All rights reserved. No reuse allowed without permission.

DNA sampling and genotyping

We used exfoliated cells that were brushed from the participants' oral mucosa for genotyping. DNA isolation was done with QIAamp DNA mini Kit (Qiagen GmbH, Hilden, Germany). Genotyping was executed with the Illumina Infinium Global Screening Array 1.0 with MDD and Psych content (Illumina, San Diego, CA, USA) at the Life & Brain facilities (Bonn, Germany) and yielded 745,747 SNPs. Filtering was conducted with PLINK 1.9 [94,95] by eliminating all SNPs with a minor allele frequency (MAF) of < 0.01, deviating from Hardy-Weinberg equilibrium (HWE) with a *p*-value of < $1*10^{-6}$, and missing data > 0.02. Participants were removed with > 0.02 missingness, sex-mismatch, and heterozygosity rate > |0.2|. A high quality (HWE $p > 0.02$, MAF > 0.2, missingness = 0) and linkage disequilibrium (LD) pruned ($r^2 = 0.1$) SNP set was used for filtering for relatedness and population structure. In pairs of related subjects, pi hat > 0.2 was used to exclude subjects randomly. Principal components (PCs) were generated to control for population stratification. Participants who deviated more than |6| standard deviations from the mean on at least one of the first 20 PCs were classified as outliers and excluded. The final data set consisted of 519 participants and 498,760 SNPs. The samples' filtered genotype data was submitted for imputation to the Michigan Imputation server [96] using the European population of the Haplotypes Reference Consortium panel (r1.1 2016; hg19) and a R^2 filter of 0.3. We chose Eagle 2.4 for phasing and Minimac4 for imputation. After a final MAF < 0.01 filtering step, 5,338,876 SNPs were available for analysis.

Polygenic scores

We generated genome-wide PGS for each participant using publicly available summary statistics for general intelligence [N = 269,867; 64]. General intelligence PGS (PGS_{GI}) were computed as weighted sums of each subject's trait-associated alleles across all SNPs using PRSice 2.1.6 [97]. Specifically, we computed best-fit PGS_{GI} that showed the strongest association with general intelligence [72,84]. We applied a *p*-value threshold (PT) for the inclusion of SNPs that was chosen empirically by carrying out multiple linear regression analyses iteratively for the range of PT $5*10^{-8}$ to 0.5 in steps of $5*10^{-5}$. The predictive power of the PGS_{GI} was assessed by the "incremental R^2" statistic [70]. Incremental R^2 indicates the increase in the coefficient of determination (R^2) when the PGS_{GI} is added as a covariate to a regression model predicting general intelligence together with a number of baseline control variables (here: age, sex, and the first four PCs of population stratification). Linear parametric methods were chosen for all statistical analyses in PRSice. Testing was two-tailed with an α-level of $p < .05$. The PGS_{GI} with the greatest predictive power, explaining the maximum amount of *g* variance, was chosen for further analyses. The best-fit threshold selected for PGS_{GI} was 0.0062, which resulted in 4,659 SNPs being included in the calculation of PGS_{GI}. PGS_{GI} explained 4.37% of variance of general intelligence in our sample ($p < .001$). A distribution of the PGS_{GI} is shown in Figure S1.

bioRxiv preprint doi: https://doi.org/10.1101/2025.01.15.633108; this version posted January 15, 2025. The copyright holder for this preprint (which was not certified by peer review) is the author/funder. All rights reserved. No reuse allowed without permission.

Acquisition and analysis of imaging data

All images were collected within one session on a Philips 3T Achieva scanner at the Bergmannsheil Hospital in Bochum, Germany, using a 32-channel head coil.

Multi-shell diffusion-weighted imaging

For the analysis of NODDI coefficients, a diffusion-weighted three-shell image was acquired using echo-planar imaging (EPI) with the following parameters: time repetition (TR) = 7652 ms; time echo (TE) = 87 ms; flip angle = 90°; 60 slices; matrix size = 112 x 112; voxel size = 2 x 2 x 2 mm; parallel imaging sensitivity encoding (SENSE) factor = 2; direction of acquisition = anterior-posterior (AP). Diffusion weighting was uniformly distributed along 120 directions (20 directions with a *b*-value of 1000 s/mm^2; 40 directions with a *b*-value of 1800 s/mm^2; 60 directions with a *b*-value of 2500 s/mm^2). We used the multiple acquisitions for standardization of structural imaging validation and evaluation toolbox (MASSIVE toolbox) [98] to generate all diffusion directions within and between shells non-collinear to each other. Additionally, eight volumes with no diffusion weighting (*b*-value of 0 s/mm^2) were acquired for the purpose of motion correction and computation of NODDI coefficients. Diffusion-weighted data was collected with reversed phase-encode directions, resulting in pairs of images with distortions going in opposite directions. Total acquisition time was 18 minutes.

Diffusion-weighted data were prepared for NODDI coefficients via a preprocessing pipeline comprising the following steps. First, images were corrected for signal drift [99] using ExploreDTI [100]. Second, we utilized the topup command from the Oxford Centre for Functional Magnetic Resonance Imaging of the Brain's (FMRIB's) Software Library (FSL) toolbox (version 6.0.7.7; https://fsl.fmrib.ox.ac.uk/fsl/docs/#/) [101,102] to estimate the susceptibility-induced off-resonance field based on pairs of images with opposite phase-encode directions. Third, the topup output was used in combination with the eddy command [103], which is also part of the FSL toolbox [101], to correct for susceptibility, eddy currents, and head movement. Importantly, we also performed outlier detection during this step to identify slices where signal had been lost due to head movement during the diffusion encoding [104].

We used the Microstructure Diffusion Toolbox (MDT; https://github.com/robbert-harms/MDT) [105,106] to compute NODDI coefficients. The advantage of MDT in comparison to the original NODDI toolbox in MATLAB [41] is that MDT is utilized on Graphics Processing Unit (GPU) cores and thus dramatically reduces estimation time. It is even faster than the AMICO toolbox [107] we used in previous studies [40,52,108]. By default, MDT uses the Offset Gaussian likelihood model and the Powell conjugate-direction optimization routine [109] for maximum likelihood estimation [105]. Specifically, we employed the implemented, three-part NODDI model of Zhang et al. [41] that distinguishes between intra-neurite, extra-neurite, and CSF

bioRxiv preprint doi: https://doi.org/10.1101/2025.01.15.633108; this version posted January 15, 2025. The copyright holder for this preprint (which was not certified by peer review) is the author/funder. All rights reserved. No reuse allowed without permission.

environments. The NODDI technique is based on a two-level approach. First, the proportion of free moving water within each voxel is analyzed based on the diffusion signal obtained by the multi-shell high-angular-resolution imaging protocol [110-112,41]. This proportion is called isotropic volume fraction and reflects the amount of isotropic diffusion with Gaussian properties that mainly characterizes regions with a focus on CSF. Second, the remaining portion of the diffusion signal is assigned to one of the complementary fractions, either intra- or extra-neurite environment [41,110,111]. The amount of intra-neurite environments is quantified as the intra-neurite volume fraction or NDI. The intra-cellular compartment represents the amount of stick-like or cylindrically symmetric diffusion that occurs when water molecules are confined by the membranes of neurites and resembles the proportion of axonal density in white matter as shown by comparison with light microscopy and electron microscopy in histological samples [110]. Extra-neurite environments in the white matter are usually full of various types of glia cells and therefore characterized by hindered diffusion [110,111,41]. A NODDI's summary statistic is the neurite ODI that quantifies angular variation of neurite orientation [41]. ODI is a measure of tortuosity that couples the intra-neurite space and the extra-neurite space and thus leads to an alignment or dispersion of the axons in the white matter [112,41]. Examples of NDI and ODI coefficient maps from a representative individual are illustrated in Figure 2 (upper-left corner).

Myelin water imaging

A previously published 32 multi-echo (ME) three-dimensional (3D) turbo gradient spin echo (GRASE) sequence with refocusing angle sweep [113,112,40,114] was acquired with the following parameters: TR = 800 ms; TE = 32 echoes at 10 ms echo spacing (ranging from 10 to 320 ms); 60 slices; partial Fourier acquisition in both phase encoding directions; matrix size = 112 x 112; voxel size = 2 x 2 x 2 mm; parallel imaging SENSE factor = 2; direction of acquisition = right-left (RL). Total acquisition time for this sequence was eight minutes.

To assess the myelin content of the white matter fiber tracts, we used an in-house algorithm [114,40] written in MATLAB (version 8.5.0.197613 (R2015a), The MathWorks Inc., Natick, MA) to construct parameter maps representing the MWF for each voxel based on the 3D ME-GRASE sequence. As described in Prasloski et al. [113] in detail, this algorithm analyzed the ME decay curves voxel by voxel using multicomponent T2 analysis with simultaneous correction for contamination of the decay curves by stimulated echoes resulting from B1 inhomogeneity and imperfect refocusing pulses. Voxelwise ME decay curves were acquired from the 3D ME-GRASE images and transformed into a continuous T2-distribution by applying a regularized non-negative least squares (NNLS) approach [115,116]. We used an extended phase graph algorithm to take possible stimulated echoes due to non-ideal refocusing pulse flip angles into consideration [117,118,113]. During the fitting procedure, a regularization factor of 1.02 was applied to increase robustness of the ill-posed fitting problem and to assure smooth

bioRxiv preprint doi: https://doi.org/10.1101/2025.01.15.633108; this version posted January 15, 2025. The copyright holder for this preprint (which was not certified by peer review) is the author/funder. All rights reserved. No reuse allowed without permission.

T2 amplitude distributions. T2 distributions were generated using 101 logarithmically spaced exponential decay base functions for echo decay with T2 values ranging from 0.01 to 2s. From the T2 distributions, the MWF was calculated for each voxel as the signal integral fraction between 10 and 40ms relative to the total T2 distribution integral (area under the curve). This resulted in whole-brain MWF maps for each subject, as exemplified in Figure 2 (upper-left corner).

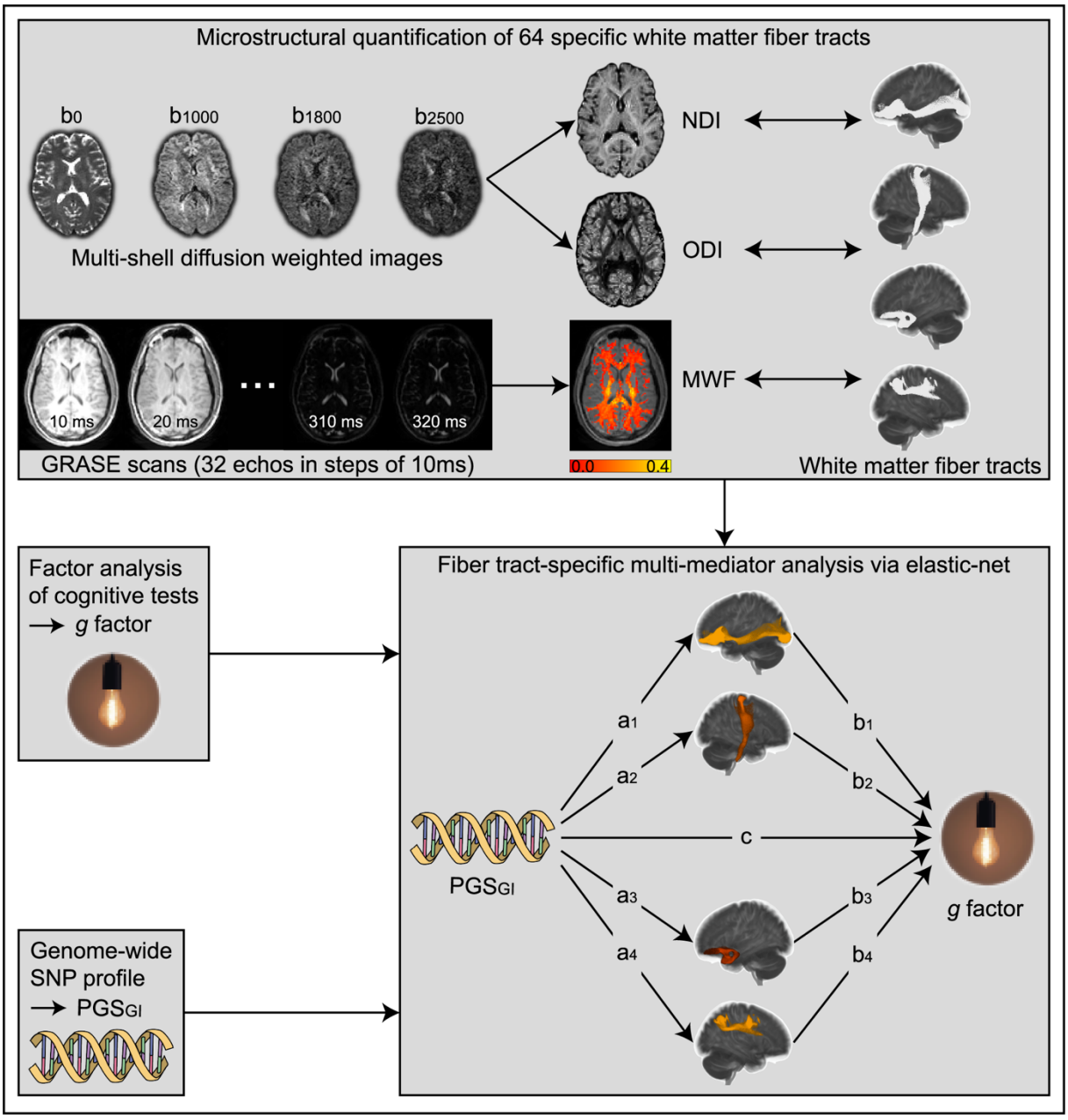

Fig. 2 Processing steps of neuroimaging and statistical analyses. Multi-shell diffusion-weighted images were used to compute neurite density and neurite orientation dispersion indices (NDI and ODI). Images resulting from the three-dimensional (3D) multi-echo (ME) turbo gradient spin echo (GRASE) sequence were used to compute the myelin water fraction (MWF) for each voxel. 64 white matter fiber tracts provided by the population-based HCP-1065 probabilistic tract atlas [119,120] were downloaded, transformed in the respective native space, and served as anatomical references for the extraction of

bioRxiv preprint doi: https://doi.org/10.1101/2025.01.15.633108; this version posted January 15, 2025. The copyright holder for this preprint (which was not certified by peer review) is the author/funder. All rights reserved. No reuse allowed without permission.

the microstructural properties NDI, ODI, and MWF. Fiber tract-specific multi-mediator analyses were performed via elastic-net regression for each microstructural property. General intelligence, quantified by the factor of general intelligence *g*, was the dependent variable, while the polygenic score of general intelligence (PGS_{GI}) was the independent variable. NDI, ODI, or MWF values of each white matter fiber tract served as mediators

Quantification of microstructural properties in white matter fiber tracts

We used 64 white matter fiber tracts provided by the population-based HCP-1065 probabilistic tract atlas [119,120], from the official website (https://brain.labsolver.org/hcp_trk_atlas.html) as NIfTI files. This atlas displays for 64 different fiber tracts for each voxel the probability of being part of the respective white matter fiber tract compiled from the tractography of 1065 subjects [119], with underlying data ("1200 Subjects Data Release") provided by the Human Connectome Project (HCP), WU-Minn Consortium (Principal Investigators: David van Essen and Kamil Ugurbil; 1U54MH091657), funded by the 16 United States National Institutes of Health (NIH) and Centers supporting the NIH Blueprint for Neuroscience Research and by the McDonnell Center for Systems Neuroscience at Washington University [121]. In a first step, fiber tracts' NIfTI files were processed using DSI Studio (https://dsi-studio.labsolver.org) [119,120]. We resized the dimensions to match the International Consortium for Brain Mapping (ICBM) 2009a Nonlinear Asymmetric NIfTI template file [122]. The threshold for the fiber tracts' probability was set at 0.50 to include only voxels that were part of major white matter tracts in at least half of the sample and exclude peripheral voxels that are more susceptible to intra- and intersubjective variability. We then binarized the fiber tracts and transformed them into a common space via FMRIB's Linear Image Registration Tool (FLIRT) [123-125]. We chose the template MNI152_T1_1mm_brain within FSL, which is derived from 152 structural images that have been nonlinearly registered into the common Montreal Neurologic Institute (MNI) 152 standard space (1 x 1 x 1 mm). Starting from the MNI 152 standard space, we used FMRIB's Nonlinear Image Registration Tool (FNIRT) [126] to nonlinearly transform the fiber tracts into the native space of the diffusion-weighted images as well as into the 3D-ME GRASE image space. Each participant's aligned fiber tracts served as anatomical references from which NODDI coefficients and MWF coefficients were extracted (see Figure 2, upper-right corner).

Statistical analyses

All statistical analyses were conducted in R Studio (version 2022.12.0.353) [127] with R version 4.2.2 (2022-10-31) [128]. The final data set included 501 participants (242 women; mean age = 27.30 years; SD = 9.22 years; 455 right-handers) as we only had usable genetic data from 519 subjects and analyzable MWF data from 539 subjects. Data points were treated as outliers if they deviated more than three interquartile ranges from the respective variable's group mean (PGS_{GI}, mean NDI of all 64 fiber tracts, mean ODI of all 64 fiber tracts, mean MWF of all 64 fiber tracts, *g*). In such cases, all data from the corresponding participant were

bioRxiv preprint doi: https://doi.org/10.1101/2025.01.15.633108; this version posted January 15, 2025. The copyright holder for this preprint (which was not certified by peer review) is the author/funder. All rights reserved. No reuse allowed without permission.

removed from analysis. No subjects were excluded from analyses concerning PGS_{GI}, NDI, MWF, and *g*, while one participant had to be excluded for analyses concerning PGS_{GI}, ODI, and *g* (500 remaining subjects).

To investigate whether a set of specific white matter fiber tracts mediates the association between PGS_{GI} (independent variable) and general intelligence (dependent variable), we used exploratory mediation analysis by regularization (see Figure 2, lower-right corner), an approach developed to identify a set of mediators from a large pool of potential mediators without testing specific theory-based and predefined hypotheses [129,130]. Confirmatory theory-based approaches in general test models that have been specified in advance, rely on *p*-values to test statistical significance, require correction for multiple comparisons with respect to many possible mediators, and tend to overfit the data in the regression context, resulting in less generalizable solutions [130-132]. In contrast, exploratory mediation analysis by regularization is based on regularization and penalization techniques [130], such as the least absolute shrinkage and selection operator (lasso) [133]. It aims to improve the generalization ability of a model and prevent overfitting [134] by applying a penalty to effect sizes, resulting in small effect sizes being pushed to zero, leaving only strong non-zero effects.

A detailed explanation of this machine learning approach is provided by Serang et al. [130]. In short, this approach is based on a two-stage process. First, all potential mediators of interest are included in a multiple mediator model which is then fit using lasso resulting in the corresponding regression weights *a* and *b* being penalized [135]. The tuning parameter of the penalty term, lambda, is typically selected by testing a range of candidate values via *k*-fold cross-validation, an approach primarily utilized to prevent overfitting [130]. The data is divided into *k* different subsets. The model is then trained on *k*-1 subsets, while the *k*th subset is used as the testing set. This is repeated *k* times so that each subset serves as the testing set once. The value of lambda chosen is the one with the best fit resulting in the lowest prediction error. Since the mediation effect of a mediator corresponds to the product of the regression parameters *a* and *b*, the effect becomes zero if either the *a* or *b* parameter of a mediator is regularized to zero by the penalty. Those mediators with non-zero values of *a* and *b* after regularization, will be considered selected as mediators. While this approach makes it possible to eliminate mediators with small effect sizes, it also means that the effect sizes of the selected mediators are close to zero due to penalization and are therefore underestimated. To eliminate this potential bias, the second step is to refit the model using only the selected mediators without any penalization [130]. This allows unbiased estimates of effect sizes to be obtained [129].

Instead of using lasso regression, we employed elastic-net regression in our analyses. Elastic-net regression results from the combination of ridge regression [136] and lasso regression [133] and is thus another form of regularized regression [137] allowing better accuracy of

bioRxiv preprint doi: https://doi.org/10.1101/2025.01.15.633108; this version posted January 15, 2025. The copyright holder for this preprint (which was not certified by peer review) is the author/funder. All rights reserved. No reuse allowed without permission.

prediction on future data and interpretation of the model due to parsimony in contrast to ordinary least squares estimates. While lasso regression can penalize a parameter to zero and is therefore suitable for models where many variables are assumed to have little or no effect on the dependent variable, ridge regression can only asymptotically shrink parameters towards zero and is therefore suitable for models where most variables are assumed to have a considerable effect on the dependent variable. Elastic-net regression is an useful approach when there are no clear, predefined hypotheses for all variables [137]. Unlike lasso regression, which tends to randomly select only one variable from a group of variables with high correlations between them, elastic-net regression outperforms lasso as it can select groups of correlated variables [137]. The latter was an important argument in our decision to use elastic-net regression instead of lasso regression.

We used the *xmed* function from the *regsem* package [138,129,130]. All variables were standardized and residualized for age, sex, age*sex, age^2, age^2*sex, and the first four PCs of population stratification. Age, sex, age^2, and their interaction effects were used as control variables, as many studies have shown age- and sex-dependent changes in microstructural properties as well as myelination [139-144]. The first four PCs of population stratification were added to control the variability of the genetic origin of the sample [145]. We calculated three mediation models, where PGS_{GI} was always the independent variable, the NDI-, ODI-, or MWF-values of the 64 white matter fiber tracts each yielded the 64 mediators, and *g* was always the dependent variable. For all mediation models, the number of cross-validation subsets was set to k = 80, the threshold for detecting non-zero mediation effects was set to 0.001 (default), and the type of regression was set to elastic-net. All coefficients were re-estimated with *lavaan* [146] to avoid biased effect sizes.

In addition to the mediation effects, we were also interested in the direct effects of PGS_{GI} on the NODDI and MWF brain properties as well as the direct effects of the NODDI and MWF brain properties on intelligence (paths *a* and paths *b*). To identify variables with non-zero effects within path *a* and path *b* regressions, we followed a similar approach and set the threshold for detecting non-zero effects to 0.01 [72]. This threshold was chosen a little more liberally, since mediation effects are considerably smaller due to the multiplication of the regularized parameters *a* and *b* with values less than one. Again, all coefficients were re-estimated with *lavaan* [146].

bioRxiv preprint doi: https://doi.org/10.1101/2025.01.15.633108; this version posted January 15, 2025. The copyright holder for this preprint (which was not certified by peer review) is the author/funder. All rights reserved. No reuse allowed without permission.

Results

Neurite density index (NDI)

The results of the multiple mediator analysis via elastic-net showed that PGS_{GI} was associated with the NDI of 28 white matter fiber tracts (see Figure 3 and supplementary Table S1). All effects were positive, indicating that higher PGS_{GI} is associated with higher NDI (path *a*) and thus higher axonal packing density. Furthermore, the NDI of 18 white matter fiber tracts was linked to the *g* score (path *b*). The association was positive for 12 white matter fiber tracts and negative for the remaining six fiber tracts. A total of six white matter fiber tracts mediated the effects of PGS_{GI} on general intelligence (path *a***b*). While the five white matter fiber tracts middle longitudinal fasciculus (left hemisphere), cingulum parahippocampal parietal (right hemisphere), uncinate fasciculus (left hemisphere), cingulum parahippocampal parietal (left hemisphere), and superior longitudinal fasciculus three (right hemisphere) showed positive mediation effects, one white matter fiber tract, namely frontal aslant tract (left hemisphere), showed a negative mediation effect.

bioRxiv preprint doi: https://doi.org/10.1101/2025.01.15.633108; this version posted January 15, 2025. The copyright holder for this preprint (which was not certified by peer review) is the author/funder. All rights reserved. No reuse allowed without permission.

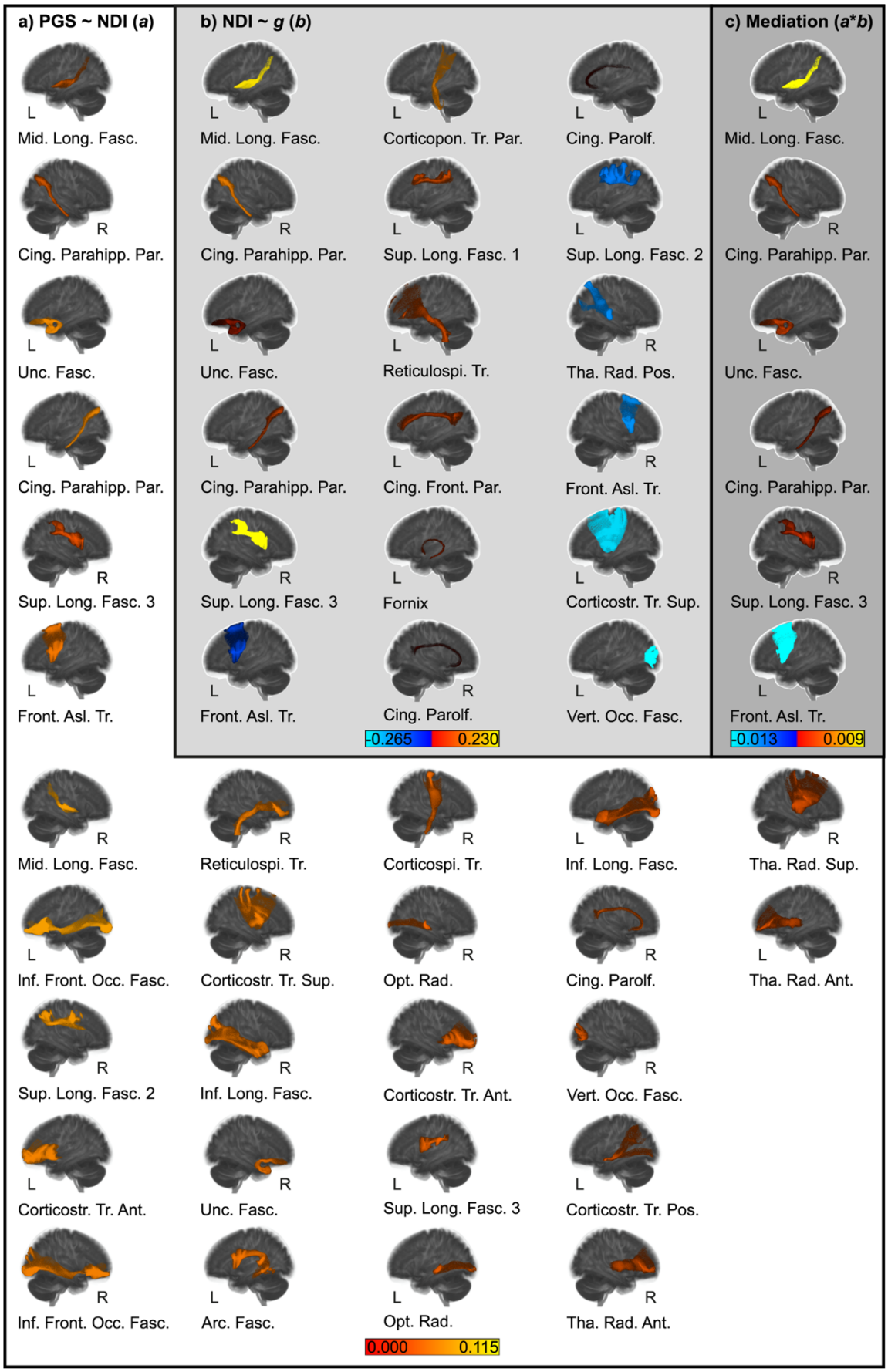

Fig. 3 Results of the multiple mediator analysis via elastic-net with neurite density index (NDI) values of 64 white matter fiber tracts as mediators. The figure shows the results from path *a* analysis (block a)

bioRxiv preprint doi: https://doi.org/10.1101/2025.01.15.633108; this version posted January 15, 2025. The copyright holder for this preprint (which was not certified by peer review) is the author/funder. All rights reserved. No reuse allowed without permission.

PGS ~ NDI (*a*)) with white background, path *b* analysis (block b) NDI ~ *g* (*b*)) with light gray background, and the mediation effects *a***b* (bock c) Mediation (*a***b*)) with gray background. White matter fiber tracts are shown in left (L) or right (R) sagittal view. Positive effects are depicted in red and yellow, negative effects are depicted in blue and light-blue. For a list of white matter fiber tracts and effect sizes see Table S1. Abbreviations: Arc. Fasc. = arcuate fasciculus; Cing. Front. Par. = cingulum frontal parietal; Cing. Parahipp. Par. = cingulum parahippocampal parietal; Cing. Parol. = cingulum parolfactory; Corticopon. Tr. Par. = corticopontine tract parietal; Corticospi. Tr. = corticospinal tract; Corticostr. Tr. Ant. = corticostriatal tract anterior; Corticostr. Tr. Pos. = corticostriatal tract posterior; Corticostr. Tr. Sup. = corticostriatal tract superior; Front. Asl. Tr. = frontal aslant tract; Inf. Front. Occ. Fasc. = inferior fronto-occipital fasciculus; Inf. Long. Fasc. = inferior longitudinal fasciculus; Mid. Long. Fasc. = middle longitudinal fasciculus; Opt. Rad. = optic radiation; Reticulospi. Tr. = reticulospinal tract; Sup. Long. Fasc. = superior longitudinal fasciculus; Tha. Rad. Ant. = thalamic radiation anterior; Tha. Rad. Pos. = thalamic radiation posterior; Tha. Rad. Sup. = thalamic radiation, superior; Unc. Fasc. = uncinate fasciculus; Vert. Occ. Fasc. = vertical occipital fasciculus

Neurite orientation dispersion index (ODI)

For the ODI metric, the elastic-net analysis showed that there was an association between PGS_{GI} and the tracts' ODI values in 16 white matter fiber tracts (see Figure 4a and supplementary Table S2). As for NDI, all effects were positive, indicating that higher PGS_{GI} is associated with higher ODI (path *a*). Higher ODI indicates a cytoarchitecture with highly dispersed neurites. The multiple mediator analysis revealed no white matter fiber tracts that showed a significant association between the tracts' ODI values and general intelligence (path *b*). Consequently, no mediators (path *a***b*) for the association between PGS_{GI} and *g* could be identified.

Myelin water fraction (MWF)

PGS_{GI} was associated with the tracts' MWF values in four white matter fiber tracts, of which two exhibited positive effects and two exhibited negative effects (see Figure 4b and supplementary Table S3). Higher PGS_{GI} was linked to higher MWF values of the corticopontine tract occipital in the left hemisphere and the reticulospinal tract in the right hemisphere, while higher PGS_{GI} went along with lower MWF values of the cingulum parahippocampal in the left hemisphere and the parietal aslant tract in the right hemisphere. Higher MWF indicates higher myelin content and thus greater myelination. As for ODI, the multiple mediator analysis revealed no white matter fiber tracts that showed a significant association between the tracts' MWF values and general intelligence (path *b*), and thus no mediators (path *a***b*) for the relation between PGS_{GI} and *g* could be identified.

bioRxiv preprint doi: https://doi.org/10.1101/2025.01.15.633108; this version posted January 15, 2025. The copyright holder for this preprint (which was not certified by peer review) is the author/funder. All rights reserved. No reuse allowed without permission.

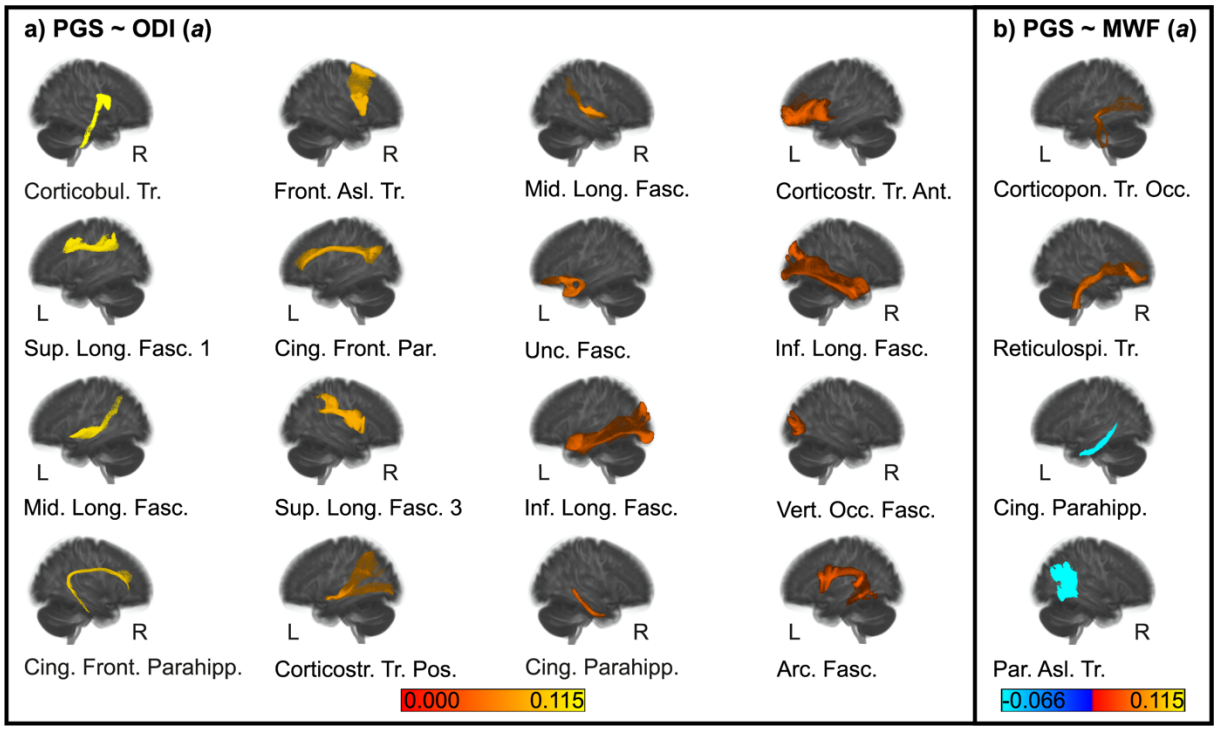

Fig. 4 Results of the multiple mediator analysis via elastic-net with neurite orientation dispersion index (ODI) values (block a) PGS ~ ODI (*a*)) or myelin water fraction (MWF) values (block b) PGS ~ MWF (*a*)) of 64 white matter fiber tracts as mediators. The figure only shows the results from paths *a* analyses, as no significant associations could be identified for paths *b* and thus also not for paths *a***b*. White matter fiber tracts are shown in left (L) or right (R) sagittal view. Positive effects are depicted in red and yellow, negative effects are depicted in blue and light-blue. For a list of white matter fiber tracts and effect sizes see Table S2 for ODI and Table S3 for MWF. Abbreviations: Arc. Fasc. = arcuate fasciculus; Cing. Front. Parahipp. = cinglum frontal parahippocampal; Cing. Front. Par. = cingulum frontal parietal; Cing. Parahipp. = cingulum parahippocampal; Corticobul. Tr. = corticobulbar tract; Corticopon. Tr. Occ. = corticopontine tract occipital; Corticostr. Tr. Ant. = corticostriatal tract anterior; Corticostr. Tr. Pos. = corticostriatal tract posterior; Front. Asl. Tr. = frontal aslant tract; Inf. Long. Fasc. = inferior longitudinal fasciculus; Mid. Long. Fasc. = middle longitudinal fasciculus; Par. Asl. Tr. = parietal aslant tract; Reticulospi. Tr. = reticulospinal tract; Sup. Long. Fasc. = superior longitudinal fasciculus; Unc. Fasc. = uncinate fasciculus; Vert. Occ. Fasc. = vertical occipital fasciculus

bioRxiv preprint doi: https://doi.org/10.1101/2025.01.15.633108; this version posted January 15, 2025. The copyright holder for this preprint (which was not certified by peer review) is the author/funder. All rights reserved. No reuse allowed without permission.

Discussion

The relation between FA values and intelligence has often been demonstrated, but it is still unclear whether it is due to greater axon density, parallel, homogenous fiber orientation distributions, or greater myelination. Using NODDI and MWF imaging data, we addressed this question and analyzed the microstructural architecture of intelligence in more detail. Furthermore, we were interested whether white matter microstructure indices are involved in the biological pathway that links genetic disposition to phenotype. Thus, we conducted for the first time mediation analyses in which we tested whether NDI, ODI, and MWF of 64 white matter fiber tracts mediated the effects of PGS_{GI} on general intelligence in a large sample of at least 500 healthy young adults. By doing so, we showed that NDI, but not ODI or MWF of white matter fiber tracts was significantly associated with general intelligence and that the NDI of six fiber tracts mediated the relation between genes and *g*.

With regard to the three hypotheses formulated by Stammen et al. [34] on possible links between brain characteristics and intelligence, our results provide clear evidence that differences in neurite density are crucial for differences in intelligence in the white matter, but not differences in neurite orientation dispersion or myelination. Since white matter mainly consists of myelinated axons [147], this means that the number or density of axons is more important for intelligent performance than their arrangement or degree of myelination. We found that 18 white matter fiber tracts showed a significant association between NDI and intelligence. For most of the fiber tracts, the correlation was positive, which fits the hypothesized explanation of Stammen et al. [34] that higher neurite density enables more parallel information processing by providing more possible pathways to think through problems simultaneously. It is a well-established finding that bigger brains are associated with higher levels of intelligence [26,148,149] and a common explanation for this phenomenon is that individuals with more cortical volume are likely to have a higher number of neurons [150]. Since most neurons have only a single axon [151], a higher axonal packing density suggests that there are more neurons in more intelligent individuals, which in turn provide them with enhanced computational power for problem solving and logical reasoning.

Among the white matter fiber tracts that showed a positive association between NDI and *g* were many fiber tracts whose FA values had already been associated with intelligence [26,15,34], namely the cingulum, uncinate fasciculus, superior longitudinal fasciculus, and fornix. This means that our results complement and specify the previous FA results in terms of neurite density. All four fiber tracts have been associated with higher cognitive functions relevant to intelligence, such as attention, cognitive control, memory, visual-spatial functions, or language [152,141,153]. We found significant positive associations between NDI and general intelligence in bilateral parahippocampal parietal, bilateral parolfactory, and left-

bioRxiv preprint doi: https://doi.org/10.1101/2025.01.15.633108; this version posted January 15, 2025. The copyright holder for this preprint (which was not certified by peer review) is the author/funder. All rights reserved. No reuse allowed without permission.

hemispheric frontal parietal subcomponents of the cingulum. Previous studies have shown that higher NDI in the (para)hippocampal cingulum was positively associated with higher cognition in a mixed sample of healthy older adults and patients with mild cognitive impairment or dementia [154], as well as with episodic memory and processing speed in healthy older adults [54]. The analysis of Raghavan et al. [154] also revealed that the superior longitudinal fasciculus had the strongest positive correlation between NDI and global cognition. This is consistent with our results of positive associations in the superior longitudinal fasciculus 1 in the left hemisphere and in the superior longitudinal fasciculus 3 in the right hemisphere. In contrast, our finding of an association between NDI and the left-hemispheric fornix was not found by Raghavan et al. [154], who averaged the values of the left and right fornix for their analysis. In addition, Coad et al. [53], who analyzed the pre- and postcommissural fornix separately, did not report any association between NDI and various cognitive factors. However, since the existing studies used different cognitive measures, defined the areas of white matter differently, and included different age groups, there are many possible factors that could have caused the different results.

Not previously noticed in FA studies on intelligence were the positive associations with the middle longitudinal fasciculus, the corticopontine tract parietal, and the reticulospinal tract in the left hemisphere. However, they were also often not included as investigated fiber tracts in previous analyses. The middle longitudinal fasciculus is an association fiber tract that connects the superior temporal gyrus with the superior parietal lobule and parietooccipital region and appears to be involved in auditory comprehension as a part of the dorsal auditory stream [141] and higher-order functions related to acoustic information [155]. The corticopontine tract runs from the cerebral cortex through the internal capsule and ends at the unilateral pontine nucleus [156]. It is part of the cerebrocerebellar system and represents an intermediate step in involving the cerebellum into the distributed neural circuits relevant to motor control, thought, and emotion [157]. The corticoreticulospinal tract originates from the premotor cortex, descends to the spinal cord and is part of the extrapyramidal system [158,159]. Although this tract is primarily associated with gross motor function, gait function, and postural stability [159,158], it may also be important for cognitive function in as yet unknown ways, as there is evidence that poor motor function is associated with accelerated cognitive decline in old age [160,161].

However, there were not only tracts whose NDI was positively associated with general intelligence, but also tracts that showed a negative relation, namely the bilateral frontal aslant tract, the left-hemispheric superior longitudinal fasciculus 2, the right-hemispheric thalamic radiation posterior, the left-hemispheric corticostriatal tract superior, and the left-hemispheric vertical occipital fasciculus. The finding that there were both positive and negative associations between white matter fiber tracts' NDI and intelligence may explain why Genç et al. [52] as well as James et al. [162] found no associations between cognition and total white matter NDI.

bioRxiv preprint doi: https://doi.org/10.1101/2025.01.15.633108; this version posted January 15, 2025. The copyright holder for this preprint (which was not certified by peer review) is the author/funder. All rights reserved. No reuse allowed without permission.

Although negative associations are less straightforward to explain, we are not the first to have revealed negative associations in circumscribed areas of the brain for structural properties that are generally positively associated with intelligence [72,74]. Furthermore, negative associations between neurite density of fiber tracts and specific skills such as single-word reading and phonological processing have already been reported for children [163]. At first, it seems counterintuitive that lower axonal density was associated with higher intelligence as it contradicts the typical finding that “bigger is better” [26,148,149]. However, it could be the result of efficient wiring and thus signal transmission of the brain so that an optimal balance between signal and noise can be achieved and no redundant or irrelevant information is passed on, which could make efficient problem solving difficult due to inefficient circuitry [52,164]. Establishing and refining efficient brain circuits may be due to regressive events such as axon pruning or synapse elimination [165], which would fit well with the neural efficiency hypothesis stating that higher intelligent individuals need to invest less cortical resources while performing cognitive tasks [166,167]. The vertical occipital fasciculus, for example, is an association fiber tract that runs vertically at the posterolateral corner of the brain and interconnects the dorsal and ventral visual stream [168]. It may be that more precise information exchange between its target regions via less dense axons is advantageous for intelligent thinking, especially since Genç et al. [72] were able to show that lower nodal efficiency and thus less efficient information exchange of the ventromedial visual area 1 with the rest of the brain is associated with higher intelligence. However, it remains to be seen whether future research efforts will be able to replicate our findings of negative associations between NDI of the mentioned fiber tracts and general intelligence in independent samples.

Our result that the orientation dispersion of no fiber tract was related to intelligence is consistent with the results of Callow et al. [55], who used the ICBM-DTI-81 white matter atlas [169-171] and reported a negative association in healthy adults only for the cerebellar peduncle, which was not included in our analysis. Our lack of an association at the level of individual fiber tracts is also well in line with the findings of Genç et al. [52] and James et al. [162], who reported no association at the global level. In contrast, Raghavan et al. [154] showed both significant positive and negative relations between ODI and global cognition in different fiber tracts, but used a mixed sample of healthy subjects and patients for their analysis.

Although it is a long-standing hypothesis that differences in myelination may underlie differences in intelligence [172], our results showed that this is not the case for general intelligence. MWF was not significantly associated with *g* in any fiber tract of the white matter. Penke et al. [20], who first demonstrated an association between myelination in terms of MTR and general intelligence, also showed in their study that this association was completely mediated by a general factor of information processing speed. Accordingly, it could be that

bioRxiv preprint doi: https://doi.org/10.1101/2025.01.15.633108; this version posted January 15, 2025. The copyright holder for this preprint (which was not certified by peer review) is the author/funder. All rights reserved. No reuse allowed without permission.

MWF is more specifically associated with processing speed than with general intelligence, especially since Page et al. [173] could show that both cognitive domains are at least partially separable with only partly overlapping cerebral correlates. Gong et al. [58] reported associations between lower MWF and steeper declines in processing speed in cognitively unimpaired adults and similar findings have been shown in patients with multiple sclerosis [174-176]. Recent results also suggest correlations of myelination with other cognitive abilities such as executive functions [59] or memory performance [60], so that the subfactors below *g* may be more strongly influenced by differences in myelination. Another way in which myelination could influence cognitive processes could be the coordination of different neuronal networks by accelerating action potentials and mediating precise timing and synchronization between neuronal ensembles [177]. However, more research is needed to understand the role of myelin architecture in functional connectivity [177].

Our finding that PGS_{GI} was significantly associated with NDI of 28, ODI of 16, and MWF of four white matter fiber tracts is in accordance with previously reported results demonstrating relations between genetic variants associated with intelligence and various brain measures [72,178,74,75]. Even if not no association was found between genes for intelligence and myelination, the low proportion of fiber tracts with an association and the lack of an association between myelination and intelligence indicate that differences in intelligence may not mainly be due to differences in myelination, as Lee et al. [70] had already assumed. This result also fits well with the fact that gene sets such as myelin sheath or regulation of myelination were not found to be significantly associated with intelligence in the GWAS used to calculate the PGS_{GI} [64]. Although Schmitt et al. [179], who used a different, less sensitive metric for myelination, found similar spatial heritability patterns for myelination and surface area, they reported that myelination, surface area, and cortical thickness were largely genetically independent in adults. Studies revealed that PGS_{GI} was associated with surface area and cortical thickness of various brain areas and that both properties of specific brain regions mediated the association between PGS_{GI} and intelligence [75,72,74]. Thus, it is conceivable that genes relevant to intelligence overlap more with genes relevant to structural morphological brain properties but less with genes relevant to myelination. However, it could also be that genes that overlap with intelligence and myelination have not yet been found in GWAS due to small effect sizes and limited sample sizes.

Interestingly, the neurite density of six fiber tracts mediated the association between PGS_{GI} and general intelligence. Five of them, namely the left-hemispheric middle longitudinal fasciculus, the bilateral cingulum parahippocampal parietal, the left-hemispheric uncinate fasciculus, and the right-hemispheric superior longitudinal fasciculus 3 exhibited positive mediation effects, which are well in line with the results of previous mediation analyses [75,72,74]. The middle longitudinal fasciculus runs from the superior temporal gyrus to the

bioRxiv preprint doi: https://doi.org/10.1101/2025.01.15.633108; this version posted January 15, 2025. The copyright holder for this preprint (which was not certified by peer review) is the author/funder. All rights reserved. No reuse allowed without permission.

superior parietal lobule and parietooccipital region [141], the cingulum parahippocampal parietal from the medial temporal lobe to the parietal and occipital lobes [180], the uncinate fasciculus from the anterior temporal lobes and amygdala to the lateral orbitofrontal and anterior portion of the prefrontal cortex [141], and the superior longitudinal fasciculus 3 from the frontal and opercular areas to the supramarginal gyrus [141]. Genç et al. [72] identified the bilaterally averaged surface area of the superior medial parietal cortex, intraparietal areas, and the posterior temporal cortex as positive mediators between PGS_{GI} and intelligence and classified all of them as part of the P-FIT model [13]. Furthermore, they found the structural network efficiency of the inferior frontal gyrus to mediate positively between genes and intelligence. Lett et al. [75] reported that the association between genetic variants and general intelligence was mediated positively by the cortical thickness and surface area of the anterior cingulate cortex, the prefrontal cortex, the insula, the medial temporal cortex, and the inferior parietal cortex. Similar mediating areas were found by Williams et al. [74]. Our results of positive mediating white matter fiber tracts thus connect regions of the brain whose morphological properties have already been identified as mediating factors between genes and intelligence and as relevant for intelligent thinking in the P-FIT model [13]. Jung and Haier [13] assumed that the entire process of reasoning depends on the fidelity of underlying white matter and we provided evidence that a higher axonal packing density of specific white matter fiber tracts is one factor that links the genetic basis of intelligence to the corresponding phenotype.

One white matter fiber tract, namely the left-hemispheric frontal aslant tract had a negative mediation effect, which was due to a negative association between its NDI and general intelligence. Negative mediation effects were also reported by Genç et al. [72], who, for example, identified the surface area of the inferior frontal sulcus as a negative mediator between genetic variants associated with educational attainment and intelligence. The frontal aslant tract runs from the pars opercularis and pars triangularis of the inferior frontal gyrus and the anterior insula to the supplementary motor area (SMA) and pre-SMA and is believed to be involved in speech planning, initiation, and production, but also kinematics and visuomotor processes [141]. As intraoperative direct electrical stimulation of the left frontal aslant tract led to stuttering [181], it could be that precise and efficient information exchange between its target regions due to lower axonal density is crucial for optimal functioning. However, the frontal aslant tract has not yet been well studied and has only recently been linked to other cognitive functions, so its role in cognition needs to be further characterized [182].

There are certain limitations to our study. Our paper is limited in its population representativeness as our sample mainly consisted of German university students who had a mean IQ score one standard deviation above average which might have impacted the associations between genetic variants, the brain, and intelligence we observed. As neurite

bioRxiv preprint doi: https://doi.org/10.1101/2025.01.15.633108; this version posted January 15, 2025. The copyright holder for this preprint (which was not certified by peer review) is the author/funder. All rights reserved. No reuse allowed without permission.

density as well as myelin content are associated with age [141,183], future studies should examine whether our results, which were limited to young adulthood, expand to other age groups or even use longitudinal designs. Furthermore, our analyses were restrained to individuals of European ancestry, thus further research is needed to investigate whether the NDI of the same white matter fiber tracts mediates the association between PGS_{GI} and general intelligence to the same degree across ancestries. As PGS_{GI} only predicted up to 5.2% of variance in general intelligence in independent samples [64], it could also be that additional white matter fiber tracts will be found when using a PGS that is based on a larger sample size and has better predictive power for intelligence. Additionally, our measures of neurite density, neurite orientation dispersion, and myelination were based on neuroimaging techniques that are limited in spatial resolution. It is known that the human brain contains different classes of axons ranging from large-diameter myelinated to small-diameter unmyelinated fibers [184,185], which could not be differentiated by the methods used. Finally, we limited our study to analyzing the relation between PGS_{GI}, white matter microstructural architecture, and general intelligence in healthy subjects. However, our type of analysis can be extended to the multitude of other PGS [186], brain correlates, and phenotypes (e.g., intelligence subfactors) in future studies and may also provide valuable insights for clinical samples.

The present paper provides the first study examining the mediating effects of the white matter microstructural indices NDI, ODI, and MWF on the association between genetic variation and general intelligence. We showed that the neurite density of specific white matter fiber tracts played a mediating role in the relation between cumulative genetic load for general intelligence and *g*-factor performance. In contrast, we found no significant associations with general intelligence for ODI and MWF. The latter was surprising, as myelination was considered a possible neurobiological correlate of intelligence. These findings are a crucial step forward in decoding the neurogenetic underpinnings of general intelligence, as they identify that the neurite density of specific white matter fiber tracts relate polygenic variation to *g*.

bioRxiv preprint doi: https://doi.org/10.1101/2025.01.15.633108; this version posted January 15, 2025. The copyright holder for this preprint (which was not certified by peer review) is the author/funder. All rights reserved. No reuse allowed without permission.

References

1. Neisser U, Boodoo G, Bouchard TJ, Boykin AW, Brody N, Ceci SJ, Halpern DF, Loehlin JC, Perloff R, Sternberg RJ, Urbina S (1996) Intelligence: Knowns and unknowns. Am Psychol 51 (2):77-101. doi:https://doi.org/10.1037/0003-066X.51.2.77
2. Deary IJ, Cox SR, Hill WD (2022) Genetic variation, brain, and intelligence differences. Mol Psychiatry (27):335-353. doi:10.1038/s41380-021-01027-y
3. Flanagan DP, Dixon SG (2013) The Cattell-Horn-Carroll theory of cognitive abilities. In: Reynolds CR, Vannest KJ, Fletcher-Janzen E (eds) Encyclopedia of Special Education. John Wiley & Sons, Inc., Hoboken, New Jersey. doi:https://doi.org/10.1002/9781118660584.ese0431
4. Spearman C (1904) "General intelligence," objectively determined and measured. Am J Psychol 15 (2):201-292
5. Schneider WJ, McGrew KS (2012) The Cattell-Horn-Carroll model of intelligence. In: Flanagan DP, Harrison PL (eds) Contemporary intellectual assessment: Theories, tests, and issues. Third Edition edn. Guilford Press, New York, pp 99-144
6. Plomin R, von Stumm S (2018) The new genetics of intelligence. Nat Rev Genet 19 (3):148-159. doi:10.1038/nrg.2017.104
7. Roth B, Becker N, Romeyke S, Schäfer S, Domnick F, Spinath FM (2015) Intelligence and school grades: A meta-analysis. Intelligence 53:118-137. doi:10.1016/j.intell.2015.09.002
8. Schmidt FL, Hunter J (2004) General mental ability in the world of work: occupational attainment and job performance. J Pers Soc Psychol 86 (1):162-173. doi:10.1037/0022-3514.86.1.162
9. Strenze T (2007) Intelligence and socioeconomic success: A meta-analytic review of longitudinal research. Intelligence 35 (5):401-426. doi:10.1016/j.intell.2006.09.004
10. Zagorsky JL (2007) Do you have to be smart to be rich? The impact of IQ on wealth, income and financial distress. Intelligence 35 (5):489-501. doi:10.1016/j.intell.2007.02.003
11. Calvin CM, Batty GD, Der G, Brett CE, Taylor A, Pattie A, Cukic I, Deary IJ (2017) Childhood intelligence in relation to major causes of death in 68 year follow-up: prospective population study. BMJ 357:j2708. doi:10.1136/bmj.j2708
12. Deary IJ (2014) The stability of intelligence from childhood to old age. Curr Dir Psychol Sci 23 (4):239-245. doi:10.1177/0963721414536905
13. Jung RE, Haier RJ (2007) The Parieto-Frontal Integration Theory (P-FIT) of intelligence: Converging neuroimaging evidence. Behav Brain Sci 30 (2):135-154. doi:10.1017/S0140525X07001185
14. Le Bihan D (2003) Looking into the functional architecture of the brain with diffusion MRI. Nat Rev Neurosci 4 (6):469-480. doi:10.1038/nrn1119
15. Genç E, Fraenz C (2021) Diffusion-weighted imaging of intelligence. In: Barbey AK, Karama S, Haier RJ (eds) The Cambridge Handbook of Intelligence and Cognitive Neuroscience. Cambridge handbooks in psychology, 1. edn. Cambridge University Press, New York, pp 191-209. doi:10.1017/9781108635462
16. Basser PJ, Pierpaoli C (1996) Microstructural and physiological features of tissues elucidated by Quantitative-Diffusion-Tensor MRI. J Magn Reson Series B 111 (3):209-219. doi:https://doi.org/10.1006/jmrb.1996.0086
17. Assaf Y, Pasternak O (2008) Diffusion tensor imaging (DTI)-based white matter mapping in brain research: a review. J Mol Neurosci 34 (1):51-61. doi:10.1007/s12031-007-0029-0
18. Tang CY, Eaves EL, Ng JC, Carpenter DM, Mai X, Schroeder DH, Condon CA, Colom R, Haier RJ (2010) Brain networks for working memory and factors of intelligence assessed in males and females with fMRI and DTI. Intelligence 38 (3):293-303. doi:10.1016/j.intell.2010.03.003
19. Booth T, Bastin ME, Penke L, Maniega SM, Murray C, Royle NA, Gow AJ, Corley J, Henderson RD, Hernandez Mdel C, Starr JM, Wardlaw JM, Deary IJ (2013) Brain white matter tract integrity and cognitive abilities in community-dwelling older people: the Lothian Birth Cohort, 1936. Neuropsychology 27 (5):595-607. doi:10.1037/a0033354

bioRxiv preprint doi: https://doi.org/10.1101/2025.01.15.633108; this version posted January 15, 2025. The copyright holder for this preprint (which was not certified by peer review) is the author/funder. All rights reserved. No reuse allowed without permission.

20. Penke L, Maniega SM, Bastin ME, Valdes Hernandez MC, Murray C, Royle NA, Starr JM, Wardlaw JM, Deary IJ (2012) Brain white matter tract integrity as a neural foundation for general intelligence. Mol Psychiatry 17 (10):1026-1030. doi:10.1038/mp.2012.66
21. Penke L, Munoz Maniega S, Murray C, Gow AJ, Hernandez MC, Clayden JD, Starr JM, Wardlaw JM, Bastin ME, Deary IJ (2010) A general factor of brain white matter integrity predicts information processing speed in healthy older people. J Neurosci 30 (22):7569-7574. doi:10.1523/JNEUROSCI.1553-10.2010
22. Kievit RA, Davis SW, Griffiths J, Correia MM, Cam C, Henson RN (2016) A watershed model of individual differences in fluid intelligence. Neuropsychologia 91:186-198. doi:10.1016/j.neuropsychologia.2016.08.008
23. Kievit RA, Davis SW, Mitchell DJ, Taylor JR, Duncan J, Cam CANRT, Henson RN, Cam CANRT (2014) Distinct aspects of frontal lobe structure mediate age-related differences in fluid intelligence and multitasking. Nat Commun 5:5658. doi:10.1038/ncomms6658
24. Kievit RA, Fuhrmann D, Borgeest GS, Simpson-Kent IL, Henson RNA (2018) The neural determinants of age-related changes in fluid intelligence: a pre-registered, longitudinal analysis in UK Biobank. Wellcome Open Res:3-38. doi:10.12688/wellcomeopenres.14241.2
25. Cremers LG, de Groot M, Hofman A, Krestin GP, van der Lugt A, Niessen WJ, Vernooij MW, Ikram MA (2016) Altered tract-specific white matter microstructure is related to poorer cognitive performance: The Rotterdam Study. Neurobiol Aging 39:108-117. doi:10.1016/j.neurobiolaging.2015.11.021
26. Cox SR, Ritchie SJ, Fawns-Ritchie C, Tucker-Drob EM, Deary IJ (2019) Structural brain imaging correlates of general intelligence in UK Biobank. Intelligence 76:101376. doi:10.1016/j.intell.2019.101376
27. Góngora D, Vega-Hernández M, Jahanshahi M, Valdés-Sosa PA, Bringas-Vega ML, CHBMP (2020) Crystallized and fluid intelligence are predicted by microstructure of specific white-matter tracts. Hum Brain Mapp 41 (4):906-916. doi:10.1002/hbm.24848
28. Holleran L, Kelly S, Alloza C, Agartz I, Andreassen OA, Arango C, Banaj N, Calhoun V, Cannon D, Carr V, Corvin A, Glahn DC, Gur R, Hong E, Hoschl C, Howells FM, James A, Janssen J, Kochunov P, Lawrie SM, Liu J, Martinez C, McDonald C, Morris D, Mothersill D, Pantelis C, Piras F, Potkin S, Rasser PE, Roalf D, Rowland L, Satterthwaite T, Schall U, Spalletta G, Spaniel F, Stein DJ, Uhlmann A, Voineskos A, Zalesky A, van Erp TGM, Turner JA, Deary IJ, Thompson PM, Jahanshad N, Donohoe G (2020) The relationship between white matter microstructure and general cognitive ability in patients with schizophrenia and healthy participants in the ENIGMA consortium. Am J Psychiatry 177 (6):537-547. doi:10.1176/appi.ajp.2019.19030225
29. Chiang MC, Barysheva M, Shattuck DW, Lee AD, Madsen SK, Avedissian C, Klunder AD, Toga AW, McMahon KL, de Zubicaray GI, Wright MJ, Srivastava A, Balov N, Thompson PM (2009) Genetics of brain fiber architecture and intellectual performance. J Neurosci 29 (7):2212-2224. doi:10.1523/JNEUROSCI.4184-08.2009
30. Dunst B, Benedek M, Koschutnig K, Jauk E, Neubauer AC (2014) Sex differences in the IQ-white matter microstructure relationship: a DTI study. Brain Cogn 91:71-78. doi:10.1016/j.bandc.2014.08.006
31. Malpas CB, Genc S, Saling MM, Velakoulis D, Desmond PM, O'Brien TJ (2016) MRI correlates of general intelligence in neurotypical adults. J Clin Neurosci 24:128-134. doi:10.1016/j.jocn.2015.07.012
32. Hidese S, Ota M, Matsuo J, Ishida I, Hiraishi M, Yokota Y, Hattori K, Yomogida Y, Kunugi H (2020) Correlation between the Wechsler adult intelligence scale- 3rd edition metrics and brain structure in healthy individuals: A whole-brain magnetic resonance imaging study. Front Hum Neurosci 14:211. doi:10.3389/fnhum.2020.00211
33. Tamnes CK, Ostby Y, Walhovd KB, Westlye LT, Due-Tonnessen P, Fjell AM (2010) Intellectual abilities and white matter microstructure in development: a diffusion tensor imaging study. Hum Brain Mapp 31 (10):1609-1625. doi:10.1002/hbm.20962
34. Stammen C, Fraenz C, Grazioplene RG, Schlüter C, Merhof V, Johnson W, Güntürkün O, DeYoung CG, Genç E (2023) Robust associations between white matter microstructure and general intelligence. Cereb Cortex 33 (11):6723-6741. doi:10.1093/cercor/bhac538

bioRxiv preprint doi: https://doi.org/10.1101/2025.01.15.633108; this version posted January 15, 2025. The copyright holder for this preprint (which was not certified by peer review) is the author/funder. All rights reserved. No reuse allowed without permission.

35. Meinert S, Nowack N, Grotegerd D, Repple J, Winter NR, Abheiden I, Enneking V, Lemke H, Waltemate L, Stein F, Brosch K, Schmitt S, Meller T, Pfarr JK, Ringwald K, Steinstrater O, Gruber M, Nenadic I, Krug A, Leehr EJ, Hahn T, Thiel K, Dohm K, Winter A, Opel N, Schubotz RI, Kircher T, Dannlowski U (2022) Association of brain white matter microstructure with cognitive performance in major depressive disorder and healthy controls: a diffusion-tensor imaging study. Mol Psychiatry 27 (2):1103-1110. doi:10.1038/s41380-021-01330-8
36. Nave KA (2010) Myelination and support of axonal integrity by glia. Nature 468 (7321):244-252. doi:10.1038/nature09614
37. Laule C, Vavasour IM, Kolind SH, Li DKB, Traboulsee TL, Moore GRW, MacKay AL (2007) Magnetic resonance imaging of myelin. Neurotherapeutics 4 (3):460-484. doi:10.1016/j.nurt.2007.05.004
38. Beaulieu C (2002) The basis of anisotropic water diffusion in the nervous system - a technical review. NMR Biomed 15 (7-8):435-455. doi:10.1002/nbm.782
39. Jones DK, Knösche TR, Turner R (2013) White matter integrity, fiber count, and other fallacies: the do's and don'ts of diffusion MRI. NeuroImage 73:239-254. doi:10.1016/j.neuroimage.2012.06.081
40. Friedrich P, Fraenz C, Schlüter C, Ocklenburg S, Madler B, Güntürkün O, Genç E (2020) The relationship between axon density, myelination, and fractional anisotropy in the human corpus callosum. Cereb Cortex 30 (4):2042-2056. doi:10.1093/cercor/bhz221
41. Zhang H, Schneider T, Wheeler-Kingshott CA, Alexander DC (2012) NODDI: practical in vivo neurite orientation dispersion and density imaging of the human brain. Neuroimage 61 (4):1000-1016. doi:10.1016/j.neuroimage.2012.03.072
42. MacKay AL, Laule C (2016) Magnetic resonance of myelin water: An in vivo marker for myelin. Brain Plast 2 (1):71-91. doi:10.3233/BPL-160033
43. Grussu F, Schneider T, Tur C, Yates RL, Tachrount M, Ianus A, Yiannakas MC, Newcombe J, Zhang H, Alexander DC, DeLuca GC, Gandini Wheeler-Kingshott CAM (2017) Neurite dispersion: a new marker of multiple sclerosis spinal cord pathology? Ann Clin Transl Neurol 4 (9):663-679. doi:10.1002/acn3.445
44. Laule C, Kozlowski P, Leung E, Li DK, Mackay AL, Moore GR (2008) Myelin water imaging of multiple sclerosis at 7 T: correlations with histopathology. Neuroimage 40 (4):1575-1580. doi:10.1016/j.neuroimage.2007.12.008
45. Laule C, Leung E, Li DKB, Traboulsee AL, Paty DW, MacKay AL, Moore GRW (2006) Myelin water imaging in multiple sclerosis: quantitative correlations with histopathology. Mult Scler 12:747-753. doi:https://doi.org/10.1177/1352458506070928
46. Laule C, Yung A, Pavolva V, Bohnet B, Kozlowski P, Hashimoto SA, Yip S, Li DK, Moore GW (2016) High-resolution myelin water imaging in post-mortem multiple sclerosis spinal cord: A case report. Mult Scler 22 (11):1485-1489. doi:10.1177/1352458515624559
47. Baadsvik EL, Weiger M, Froidevaux R, Faigle W, Ineichen BV, Pruessmann KP (2023) Mapping the myelin bilayer with short-T(2) MRI: Methods validation and reference data for healthy human brain. Magn Reson Med 89 (2):665-677. doi:10.1002/mrm.29481
48. Meyers SM, Vavasour IM, Madler B, Harris T, Fu E, Li DK, Traboulsee AL, MacKay AL, Laule C (2013) Multicenter measurements of myelin water fraction and geometric mean T2: Intra- and intersite reproducibility. J Magn Reson Imaging 38 (6):1445-1453. doi:10.1002/jmri.24106
49. Borich MR, Mackay AL, Vavasour IM, Rauscher A, Boyd LA (2013) Evaluation of white matter myelin water fraction in chronic stroke. Neuroimage Clin 2:569-580. doi:10.1016/j.nicl.2013.04.006
50. Vargas WS, Monohan E, Pandya S, Raj A, Vartanian T, Nguyen TD, Hurtado Rua SM, Gauthier SA (2015) Measuring longitudinal myelin water fraction in new multiple sclerosis lesions. Neuroimage Clin 9:369-375. doi:10.1016/j.nicl.2015.09.003
51. Vavasour IM, Clark CM, Li DK, Mackay AL (2006) Reproducibility and reliability of MR measurements in white matter: Clinical implications. Neuroimage 32 (2):637-642. doi:10.1016/j.neuroimage.2006.03.036
52. Genç E, Fraenz C, Schlüter C, Friedrich P, Hossiep R, Voelkle MC, Ling JM, Güntürkün O, Jung RE (2018) Diffusion markers of dendritic density and arborization in gray matter predict differences in intelligence. Nat Commun 9 (1):1905. doi:10.1038/s41467-018-04268-8

bioRxiv preprint doi: https://doi.org/10.1101/2025.01.15.633108; this version posted January 15, 2025. The copyright holder for this preprint (which was not certified by peer review) is the author/funder. All rights reserved. No reuse allowed without permission.

53. Coad BM, Craig E, Louch R, Aggleton JP, Vann SD, Metzler-Baddeley C (2020) Precommissural and postcommissural fornix microstructure in healthy aging and cognition. Brain and Neuroscience Advances 4:1-12. doi:10.1177/2398212819899316
54. Gozdas E, Fingerhut H, Dacorro L, Bruno JL, Hosseini SMH (2021) Neurite imaging reveals widespread alterations in gray and white matter neurite morphology in healthy aging and amnestic mild cognitive impairment. Cerebral Cortex 31 (12):5570-5578. doi:10.1093/cercor/bhab180
55. Callow DD, Purcell JJ, Won J, Smith JC (2022) Neurite dispersion and density mediates the relationship between cardiorespiratory fitness and cognition in healthy younger adults. Neuropsychologia 169:108207. doi:10.1016/j.neuropsychologia.2022.108207
56. Gareau PJ, Rutt BK, Karlik SJ, Mitchell JR (2000) Magnetization transfer and multicomponent T2 relaxation measurements with histopathologic correlation in an experimental model of MS. Journal of Magnetic Resonance Imaging 11 (6):586-595. doi:10.1002/1522-2586(200006)11:6<586::Aid-jmri3>3.0.Co;2-v
57. Vavasour IM, Laule C, Li DK, Traboulsee AL, MacKay AL (2011) Is the magnetization transfer ratio a marker for myelin in multiple sclerosis? J Magn Reson Imaging 33 (3):713-718. doi:10.1002/jmri.22441
58. Gong Z, Bilgel M, Resnick SM, An Y, Bouhrara M (2023) White matter myelination is associated with longitudinal changes in processing speed in normative aging. Alzheimer's & Dementia 19 (S16). doi:10.1002/alz.076956
59. Gong Z, Bilgel M, Kiely M, Triebswetter C, Ferrucci L, Resnick SM, Spencer RG, Bouhrara M (2023) Lower myelin content is associated with more rapid cognitive decline among cognitively unimpaired individuals. Alzheimers Dement 19 (7):3098-3107. doi:10.1002/alz.12968
60. Mendez Colmenares A, Thomas ML, Anderson C, Arciniegas DB, Calhoun V, Choi IY, Kramer AF, Li K, Lee J, Lee P, Burzynska AZ (2024) Testing the structural disconnection hypothesis: Myelin content correlates with memory in healthy aging. Neurobiol Aging 141:21-33. doi:10.1016/j.neurobiolaging.2024.05.013
61. Haworth CM, Wright MJ, Luciano M, Martin NG, de Geus EJ, van Beijsterveldt CE, Bartels M, Posthuma D, Boomsma DI, Davis OS, Kovas Y, Corley RP, Defries JC, Hewitt JK, Olson RK, Rhea SA, Wadsworth SJ, Iacono WG, McGue M, Thompson LA, Hart SA, Petrill SA, Lubinski D, Plomin R (2010) The heritability of general cognitive ability increases linearly from childhood to young adulthood. Mol Psychiatry 15 (11):1112-1120. doi:10.1038/mp.2009.55
62. Polderman TJ, Benyamin B, de Leeuw CA, Sullivan PF, van Bochoven A, Visscher PM, Posthuma D (2015) Meta-analysis of the heritability of human traits based on fifty years of twin studies. Nat Genet 47 (7):702-709. doi:10.1038/ng.3285
63. Choi SW, Mak TS, O'Reilly PF (2020) Tutorial: a guide to performing polygenic risk score analyses. Nat Protoc 15 (9):2759-2772. doi:10.1038/s41596-020-0353-1
64. Savage JE, Jansen PR, Stringer S, Watanabe K, Bryois J, de Leeuw CA, Nagel M, Awasthi S, Barr PB, Coleman JRI, Grasby KL, Hammerschlag AR, Kaminski JA, Karlsson R, Krapohl E, Lam M, Nygaard M, Reynolds CA, Trampush JW, Young H, Zabaneh D, Hagg S, Hansell NK, Karlsson IK, Linnarsson S, Montgomery GW, Munoz-Manchado AB, Quinlan EB, Schumann G, Skene NG, Webb BT, White T, Arking DE, Avramopoulos D, Bilder RM, Bitsios P, Burdick KE, Cannon TD, Chiba-Falek O, Christoforou A, Cirulli ET, Congdon E, Corvin A, Davies G, Deary IJ, DeRosse P, Dickinson D, Djurovic S, Donohoe G, Conley ED, Eriksson JG, Espeseth T, Freimer NA, Giakoumaki S, Giegling I, Gill M, Glahn DC, Hariri AR, Hatzimanolis A, Keller MC, Knowles E, Koltai D, Konte B, Lahti J, Le Hellard S, Lencz T, Liewald DC, London E, Lundervold AJ, Malhotra AK, Melle I, Morris D, Need AC, Ollier W, Palotie A, Payton A, Pendleton N, Poldrack RA, Raikkonen K, Reinvang I, Roussos P, Rujescu D, Sabb FW, Scult MA, Smeland OB, Smyrnis N, Starr JM, Steen VM, Stefanis NC, Straub RE, Sundet K, Tiemeier H, Voineskos AN, Weinberger DR, Widen E, Yu J, Abecasis G, Andreassen OA, Breen G, Christiansen L, Debrabant B, Dick DM, Heinz A, Hjerling-Leffler J, Ikram MA, Kendler KS, Martin NG, Medland SE, Pedersen NL, Plomin R, Polderman TJC, Ripke S, van der Sluis S, Sullivan PF, Vrieze SI, Wright MJ, Posthuma D (2018) Genome-

bioRxiv preprint doi: https://doi.org/10.1101/2025.01.15.633108; this version posted January 15, 2025. The copyright holder for this preprint (which was not certified by peer review) is the author/funder. All rights reserved. No reuse allowed without permission.

wide association meta-analysis in 269,867 individuals identifies new genetic and functional links to intelligence. Nat Genet 50 (7):912-919. doi:10.1038/s41588-018-0152-6
65. Davies G, Lam M, Harris SE, Trampush JW, Luciano M, Hill WD, Hagenaars SP, Ritchie SJ, Marioni RE, Fawns-Ritchie C, Liewald DCM, Okely JA, Ahola-Olli AV, Barnes CLK, Bertram L, Bis JC, Burdick KE, Christoforou A, DeRosse P, Djurovic S, Espeseth T, Giakoumaki S, Giddaluru S, Gustavson DE, Hayward C, Hofer E, Ikram MA, Karlsson R, Knowles E, Lahti J, Leber M, Li S, Mather KA, Melle I, Morris D, Oldmeadow C, Palviainen T, Payton A, Pazoki R, Petrovic K, Reynolds CA, Sargurupremraj M, Scholz M, Smith JA, Smith AV, Terzikhan N, Thalamuthu A, Trompet S, van der Lee SJ, Ware EB, Windham BG, Wright MJ, Yang J, Yu J, Ames D, Amin N, Amouyel P, Andreassen OA, Armstrong NJ, Assareh AA, Attia JR, Attix D, Avramopoulos D, Bennett DA, Böhmer AC, Boyle PA, Brodaty H, Campbell H, Cannon TD, Cirulli ET, Congdon E, Conley ED, Corley J, Cox SR, Dale AM, Dehghan A, Dick D, Dickinson D, Eriksson JG, Evangelou E, Faul JD, Ford I, Freimer NA, Gao H, Giegling I, Gillespie NA, Gordon SD, Gottesman RF, Griswold ME, Gudnason V, Harris TB, Hartmann AM, Hatzimanolis A, Heiss G, Holliday EG, Joshi PK, Kähönen M, Kardia SLR, Karlsson I, Kleineidam L, Knopman DS, Kochan NA, Konte B, Kwok JB, Le Hellard S, Lee T, Lehtimäki T, Li S-C, Lill CM, Liu T, Koini M, London E, Longstreth WT, Lopez OL, Loukola A, Luck T, Lundervold AJ, Lundquist A, Lyytikäinen L-P, Martin NG, Montgomery GW, Murray AD, Need AC, Noordam R, Nyberg L, Ollier W, Papenberg G, Pattie A, Polasek O, Poldrack RA, Psaty BM, Reppermund S, Riedel-Heller SG, Rose RJ, Rotter JI, Roussos P, Rovio SP, Saba Y, Sabb FW, Sachdev PS, Satizabal CL, Schmid M, Scott RJ, Scult MA, Simino J, Slagboom PE, Smyrnis N, Soumaré A, Stefanis NC, Stott DJ, Straub RE, Sundet K, Taylor AM, Taylor KD, Tzoulaki I, Tzourio C, Uitterlinden A, Vitart V, Voineskos AN, Kaprio J, Wagner M, Wagner H, Weinhold L, Wen KH, Widen E, Yang Q, Zhao W, Adams HHH, Arking DE, Bilder RM, Bitsios P, Boerwinkle E, Chiba-Falek O, Corvin A, De Jager PL, Debette S, Donohoe G, Elliott P, Fitzpatrick AL, Gill M, Glahn DC, Hägg S, Hansell NK, Hariri AR, Ikram MK, Jukema JW, Vuoksimaa E, Keller MC, Kremen WS, Launer L, Lindenberger U, Palotie A, Pedersen NL, Pendleton N, Porteous DJ, Räikkönen K, Raitakari OT, Ramirez A, Reinvang I, Rudan I, Dan R, Schmidt R, Schmidt H, Schofield PW, Schofield PR, Starr JM, Steen VM, Trollor JN, Turner ST, Van Duijn CM, Villringer A, Weinberger DR, Weir DR, Wilson JF, Malhotra A, McIntosh AM, Gale CR, Seshadri S, Mosley TH, Bressler J, Lencz T, Deary IJ (2018) Study of 300,486 individuals identifies 148 independent genetic loci influencing general cognitive function. Nature Communications 9 (1). doi:10.1038/s41467-018-04362-x
66. Zhao B, Zhang J, Ibrahim JG, Luo T, Santelli RC, Li Y, Li T, Shan Y, Zhu Z, Zhou F, Liao H, Nichols TE, Zhu H (2021) Large-scale GWAS reveals genetic architecture of brain white matter microstructure and genetic overlap with cognitive and mental health traits (n = 17,706). Mol Psychiatry 26 (8):3943-3955. doi:10.1038/s41380-019-0569-z
67. Fan CC, Loughnan R, Makowski C, Pecheva D, Chen CH, Hagler DJ, Jr., Thompson WK, Parker N, van der Meer D, Frei O, Andreassen OA, Dale AM (2022) Multivariate genome-wide association study on tissue-sensitive diffusion metrics highlights pathways that shape the human brain. Nat Commun 13 (1):2423. doi:10.1038/s41467-022-30110-3
68. Zhao B, Li T, Yang Y, Wang X, Luo T, Shan Y, Zhu Z, Xiong D, Hauberg ME, Bendl J, Fullard JF, Roussos P, Li Y, Stein JL, Zhu H (2021) Common genetic variation influencing human white matter microstructure. Science 372 (6548). doi:10.1126/science.abf3736
69. Hill WD, Marioni RE, Maghzian O, Ritchie SJ, Hagenaars SP, McIntosh AM, Gale CR, Davies G, Deary IJ (2019) A combined analysis of genetically correlated traits identifies 187 loci and a role for neurogenesis and myelination in intelligence. Molecular Psychiatry 24 (2):169-181. doi:10.1038/s41380-017-0001-5
70. Lee JJ, Wedow R, Okbay A, Kong E, Maghzian O, Zacher M, Nguyen-Viet TA, Bowers P, Sidorenko J, Karlsson Linner R, Fontana MA, Kundu T, Lee C, Li H, Li R, Royer R, Timshel PN, Walters RK, Willoughby EA, Yengo L, andMe Research T, Cogent, Social Science Genetic Association C, Alver M, Bao Y, Clark DW, Day FR, Furlotte NA, Joshi PK, Kemper KE, Kleinman A, Langenberg C, Magi R, Trampush JW, Verma SS, Wu Y, Lam M, Zhao JH, Zheng Z, Boardman JD, Campbell H, Freese J, Harris KM, Hayward C, Herd P, Kumari M, Lencz T, Luan J, Malhotra AK, Metspalu A, Milani L, Ong KK, Perry JRB, Porteous DJ,

bioRxiv preprint doi: https://doi.org/10.1101/2025.01.15.633108; this version posted January 15, 2025. The copyright holder for this preprint (which was not certified by peer review) is the author/funder. All rights reserved. No reuse allowed without permission.

Ritchie MD, Smart MC, Smith BH, Tung JY, Wareham NJ, Wilson JF, Beauchamp JP, Conley DC, Esko T, Lehrer SF, Magnusson PKE, Oskarsson S, Pers TH, Robinson MR, Thom K, Watson C, Chabris CF, Meyer MN, Laibson DI, Yang J, Johannesson M, Koellinger PD, Turley P, Visscher PM, Benjamin DJ, Cesarini D (2018) Gene discovery and polygenic prediction from a genome-wide association study of educational attainment in 1.1 million individuals. Nat Genet 50 (8):1112-1121. doi:10.1038/s41588-018-0147-3
71. Mitchell BL, Cuellar-Partida G, Grasby KL, Campos AI, Strike LT, Hwang LD, Okbay A, Thompson PM, Medland SE, Martin NG, Wright MJ, Renteria ME (2020) Educational attainment polygenic scores are associated with cortical total surface area and regions important for language and memory. Neuroimage 212:116691. doi:10.1016/j.neuroimage.2020.116691
72. Genç E, Metzen D, Fraenz C, Schlüter C, Voelkle MC, Arning L, Streit F, Nguyen HP, Güntürkün O, Ocklenburg S, Kumsta R (2023) Structural architecture and brain network efficiency link polygenic scores to intelligence. Hum Brain Mapp:1-18. doi:10.1002/hbm.26286
73. Elliott ML, Belsky DW, Anderson K, Corcoran DL, Ge T, Knodt A, Prinz JA, Sugden K, Williams B, Ireland D, Poulton R, Caspi A, Holmes A, Moffitt T, Hariri AR (2019) A polygenic score for higher educational attainment is associated with larger brains. Cereb Cortex 29 (8):3496-3504. doi:10.1093/cercor/bhy219
74. Williams CM, Peyre H, Ramus F (2023) Brain volumes, thicknesses, and surface areas as mediators of genetic factors and childhood adversity on intelligence. Cereb Cortex 33 (10):5885-5895. doi:10.1093/cercor/bhac468
75. Lett TA, Vogel BO, Ripke S, Wackerhagen C, Erk S, Awasthi S, Trubetskoy V, Brandl EJ, Mohnke S, Veer IM, Nothen MM, Rietschel M, Degenhardt F, Romanczuk-Seiferth N, Witt SH, Banaschewski T, Bokde ALW, Buchel C, Quinlan EB, Desrivieres S, Flor H, Frouin V, Garavan H, Gowland P, Ittermann B, Martinot JL, Martinot MP, Nees F, Papadopoulos-Orfanos D, Paus T, Poustka L, Frohner JH, Smolka MN, Whelan R, Schumann G, Tost H, Meyer-Lindenberg A, Heinz A, Walter H, consortium I (2020) Cortical surfaces mediate the relationship between polygenic scores for intelligence and general intelligence. Cereb Cortex 30 (4):2707-2718. doi:10.1093/cercor/bhz270
76. Oldfield RC (1971) The assessment and analysis of handedness: The Edinburgh Inventory. Neuropsychologia 9 (1):97-113. doi:https://doi.org/10.1016/0028-3932(71)90067-4
77. Liepmann D, Beauducel A, Brocke B, Amthauer R (2007) Intelligenz-Struktur-Test 2000 R (I-S-T 2000 R). Manual., vol 2., erweiterte und überarbeitete Auflage. Hogrefe, Göttingen (Germany)
78. Erdodi LA, Abeare CA, Lichtenstein JD, Tyson BT, Kucharski B, Zuccato BG, Roth RM (2017) Wechsler Adult Intelligence Scale-Fourth Edition (WAIS-IV) processing speed scores as measures of noncredible responding: The third generation of embedded performance validity indicators. Psychol Assess 29 (2):148-157. doi:10.1037/pas0000319
79. Hossiep R, Hasella M, Turck D (2001) BOMAT-advanced-short version: Bochumer Matrizentest. Hogrefe, Göttingen (Germany)
80. Jaeggi SM, Buschkuehl M, Jonides J, Perrig WJ (2008) Improving fluid intelligence with training on working memory. Proc Natl Acad Sci U S A 105 (19):6829-6833. doi:10.1073/pnas.0801268105
81. Oelhafen S, Nikolaidis A, Padovani T, Blaser D, Koenig T, Perrig WJ (2013) Increased parietal activity after training of interference control. Neuropsychologia 51 (13):2781-2790. doi:10.1016/j.neuropsychologia.2013.08.012
82. Fraenz C, Schlüter C, Friedrich P, Jung RE, Güntürkün O, Genç E (2021) Interindividual differences in matrix reasoning are linked to functional connectivity between brain regions nominated by Parieto-Frontal Integration Theory. Intelligence 87:101545. doi:https://doi.org/10.1016/j.intell.2021.101545
83. Genç E, Fraenz C, Schlüter C, Friedrich P, Voelkle MC, Hossiep R, Güntürkün O (2019) The neural architecture of general knowledge. EJP 33 (5):589-605. doi:10.1002/per.2217
84. Genç E, Schlüter C, Fraenz C, Arning L, Metzen D, Nguyen HP, Voelkle MC, Streit F, Güntürkün O, Kumsta R, Ocklenburg S (2021) Polygenic scores for cognitive abilities and

bioRxiv preprint doi: https://doi.org/10.1101/2025.01.15.633108; this version posted January 15, 2025. The copyright holder for this preprint (which was not certified by peer review) is the author/funder. All rights reserved. No reuse allowed without permission.

their association with different aspects of general intelligence—A deep phenotyping approach. Mol Neurobiol 58:4145-4156. doi:10.1007/s12035-021-02398-7
85. Raven JC, Court JH, Raven J (1990) Coloured progressive matrices. Manual for Raven's Progressive Matrices and Vocabulary Scales. Oxford Psychologists Press, Oxford (United Kingdom)
86. Hossiep R, Schulte M (2008) BOWIT: Bochumer Wissenstest. Hogrefe, Göttingen (Germany)
87. Oswald WD, Roth E (1987) Der Zahlen-Verbindungs-Test (ZVT). Hogrefe Verlag für Psychologie, Göttingen (Germany)
88. Johnson W, Bouchard TJ, Krueger RF, McGue M, Gottesman II (2004) Just one g: consistent results from three test batteries. Intelligence 32 (1):95-107. doi:10.1016/s0160-2896(03)00062-x
89. Johnson W, Nijenhuis Jt, Bouchard TJ (2008) Still just 1 g: Consistent results from five test batteries. Intelligence 36 (1):81-95. doi:10.1016/j.intell.2007.06.001
90. Hu Lt, Bentler PM (1999) Cutoff criteria for fit indexes in covariance structure analysis: Conventional criteria versus new alternatives. Struct Equ Model 6 (1):1-55. doi:10.1080/10705519909540118
91. Bentler PM, Bonett G (1980) Significance tests and goodness of fit in the analysis of covariance structures. Psychol Bull 88 (3):588-606. doi:10.1037/0033-2909.88.3.588
92. Jöreskog KG (1969) A general approach to confirmatory maximum likelihood factor analysis. Psychometrika 34 (2):183-202. doi:https://psycnet.apa.org/doi/10.1007/BF02289343
93. Wilcox RR (1997) Introduction to robust estimation and hypothesis testing. Academic Press, San Diego
94. Chang CC, Chow CC, Tellier LC, Vattikuti S, Purcell SM, Lee JJ (2015) Second-generation PLINK: rising to the challenge of larger and richer datasets. Gigascience 4:7. doi:10.1186/s13742-015-0047-8
95. Purcell S, Chang C PLINK 1.9. www.cog-genomics.org/plink/1.9/.
96. Das S, Forer L, Schonherr S, Sidore C, Locke AE, Kwong A, Vrieze SI, Chew EY, Levy S, McGue M, Schlessinger D, Stambolian D, Loh PR, Iacono WG, Swaroop A, Scott LJ, Cucca F, Kronenberg F, Boehnke M, Abecasis GR, Fuchsberger C (2016) Next-generation genotype imputation service and methods. Nat Genet 48 (10):1284-1287. doi:10.1038/ng.3656
97. Choi SW, O'Reilly PF (2019) PRSice-2: Polygenic Risk Score software for biobank-scale data. Gigascience 8 (7). doi:10.1093/gigascience/giz082
98. Froeling M, Tax CMW, Vos SB, Luijten PR, Leemans A (2017) "MASSIVE" brain dataset: Multiple acquisitions for standardization of structural imaging validation and evaluation. Magn Reson Med 77 (5):1797-1809. doi:10.1002/mrm.26259
99. Vos SB, Tax CM, Luijten PR, Ourselin S, Leemans A, Froeling M (2017) The importance of correcting for signal drift in diffusion MRI. Magn Reson Med 77 (1):285-299. doi:10.1002/mrm.26124
100. Leemans A, Jeurissen B, Sijbers J, Jones DK (2009) ExploreDTI: a graphical toolbox for processing, analyzing, and visualizing diffusion MR data. Proc Intl Soc Mag Reson Med 17:3537
101. Smith SM, Jenkinson M, Woolrich MW, Beckmann CF, Behrens TE, Johansen-Berg H, Bannister PR, De Luca M, Drobnjak I, Flitney DE, Niazy RK, Saunders J, Vickers J, Zhang Y, De Stefano N, Brady JM, Matthews PM (2004) Advances in functional and structural MR image analysis and implementation as FSL. NeuroImage 23 Suppl 1:S208-S219. doi:10.1016/j.neuroimage.2004.07.051
102. Andersson JL, Skare S, Ashburner J (2003) How to correct susceptibility distortions in spin-echo echo-planar images: application to diffusion tensor imaging. Neuroimage 20 (2):870-888. doi:10.1016/S1053-8119(03)00336-7
103. Andersson JLR, Sotiropoulos SN (2016) An integrated approach to correction for off-resonance effects and subject movement in diffusion MR imaging. Neuroimage 125:1063-1078. doi:10.1016/j.neuroimage.2015.10.019
104. Andersson JLR, Graham MS, Zsoldos E, Sotiropoulos SN (2016) Incorporating outlier detection and replacement into a non-parametric framework for movement and distortion

bioRxiv preprint doi: https://doi.org/10.1101/2025.01.15.633108; this version posted January 15, 2025. The copyright holder for this preprint (which was not certified by peer review) is the author/funder. All rights reserved. No reuse allowed without permission.

correction of diffusion MR images. Neuroimage 141:556-572. doi:10.1016/j.neuroimage.2016.06.058
105. Harms RL, Fritz FJ, Tobisch A, Goebel R, Roebroeck A (2017) Robust and fast nonlinear optimization of diffusion MRI microstructure models. Neuroimage 155:82-96. doi:10.1016/j.neuroimage.2017.04.064
106. Harms RL, Roebroeck A (2018) Robust and fast Markov Chain Monte Carlo sampling of diffusion MRI microstructure models. Front Neuroinform 12:97. doi:10.3389/fninf.2018.00097
107. Daducci A, Canales-Rodriguez EJ, Zhang H, Dyrby TB, Alexander DC, Thiran JP (2015) Accelerated Microstructure Imaging via Convex Optimization (AMICO) from diffusion MRI data. Neuroimage 105:32-44. doi:10.1016/j.neuroimage.2014.10.026
108. Schlüter C, Fraenz C, Friedrich P, Güntürkün O, Genç E (2022) Neurite density imaging in amygdala nuclei reveals interindividual differences in neuroticism. Hum Brain Mapp 43 (6):2051-2063. doi:10.1002/hbm.25775
109. Powell MJD (1964) An efficient method for finding the minimum of a function of several variables without calculating derivatives. Comput J 7 (2):155-162. doi:https://doi.org/10.1093/comjnl/7.2.155
110. Jespersen SN, Bjarkam CR, Nyengaard JR, Chakravarty MM, Hansen B, Vosegaard T, Ostergaard L, Yablonskiy D, Nielsen NC, Vestergaard-Poulsen P (2010) Neurite density from magnetic resonance diffusion measurements at ultrahigh field: comparison with light microscopy and electron microscopy. Neuroimage 49 (1):205-216. doi:10.1016/j.neuroimage.2009.08.053
111. Jespersen SN, Leigland LA, Cornea A, Kroenke CD (2012) Determination of axonal and dendritic orientation distributions within the developing cerebral cortex by diffusion tensor imaging. IEEE Trans Med Imaging 31 (1):16-32. doi:10.1109/TMI.2011.2162099
112. Billiet T, Vandenbulcke M, Madler B, Peeters R, Dhollander T, Zhang H, Deprez S, Van den Bergh BR, Sunaert S, Emsell L (2015) Age-related microstructural differences quantified using myelin water imaging and advanced diffusion MRI. Neurobiol Aging 36 (6):2107-2121. doi:10.1016/j.neurobiolaging.2015.02.029
113. Prasloski T, Rauscher A, MacKay AL, Hodgson M, Vavasour IM, Laule C, Mädler B (2012) Rapid whole cerebrum myelin water imaging using a 3D GRASE sequence. NeuroImage 63 (1):533-539. doi:10.1016/j.neuroimage.2012.06.064
114. Ocklenburg S, Anderson C, Gerding WM, Fraenz C, Schluter C, Friedrich P, Raane M, Madler B, Schlaffke L, Arning L, Epplen JT, Gunturkun O, Beste C, Genc E (2019) Myelin water fraction imaging reveals hemispheric asymmetries in human white matter that are associated with genetic variation in PLP1. Mol Neurobiol 56 (6):3999-4012. doi:10.1007/s12035-018-1351-y
115. Whittal KP, MacKay AL (1989) Quantitative interpretation of NMR relaxation data. J Magn Reson 84 (1):134-152. doi:https://doi.org/10.1016/0022-2364(89)90011-5
116. Whittall KP, MacKay AL, Graeb DA, Nugent RA, Li DK, Paty DW (1997) In vivo measurement of T2 distributions and water contents in normal human brain. Magn Reson Med 37 (1):34-43. doi:10.1002/mrm.1910370107
117. Hennig J (1988) Multiecho imaging sequences with low refocusing flip angles. J Magn Reson 78 (3):397-407. doi:https://doi.org/10.1016/0022-2364(88)90128-X
118. Hennig J, Weigel M, Scheffler K (2003) Multiecho sequences with variable refocusing flip angles: optimization of signal behavior using smooth transitions between pseudo steady states (TRAPS). Magn Reson Med 49 (3):527-535. doi:10.1002/mrm.10391
119. Yeh FC (2022) Population-based tract-to-region connectome of the human brain and its hierarchical topology. Nat Commun 13 (1):4933. doi:10.1038/s41467-022-32595-4
120. Yeh FC, Panesar S, Fernandes D, Meola A, Yoshino M, Fernandez-Miranda JC, Vettel JM, Verstynen T (2018) Population-averaged atlas of the macroscale human structural connectome and its network topology. Neuroimage 178:57-68. doi:10.1016/j.neuroimage.2018.05.027
121. van Essen DC, Smith SM, Barch DM, Behrens TE, Yacoub E, Ugurbil K, Consortium WU-MH (2013) The WU-Minn Human Connectome Project: an overview. NeuroImage 80:62-79. doi:10.1016/j.neuroimage.2013.05.041

bioRxiv preprint doi: https://doi.org/10.1101/2025.01.15.633108; this version posted January 15, 2025. The copyright holder for this preprint (which was not certified by peer review) is the author/funder. All rights reserved. No reuse allowed without permission.

122. Fonov V, Evans AC, Botteron K, Almli CR, McKinstry RC, Collins DL, Brain Development Cooperative G (2011) Unbiased average age-appropriate atlases for pediatric studies. Neuroimage 54 (1):313-327. doi:10.1016/j.neuroimage.2010.07.033
123. Jenkinson M, Bannister P, Brady M, Smith S (2002) Improved optimization for the robust and accurate linear registration and motion correction of brain images. NeuroImage 17 (2):825-841. doi:10.1006/nimg.2002.1132
124. Jenkinson M, Smith SM (2001) A global optimisation method for robust affine registration of brain images. Med Image Anal 5 (2):143-156. doi:https://doi.org/10.1016/s1361-8415(01)00036-6
125. Greve DN, Fischl B (2009) Accurate and robust brain image alignment using boundary-based registration. Neuroimage 48 (1):63-72. doi:10.1016/j.neuroimage.2009.06.060
126. Andersson JLR, Jenkinson M, Smith SM (2007) Non-linear registration aka Spatial normalisation. FMRIB technical report TR07JA2.
127. Posit team (2022) RStudio: Integrated Development Environment for R. 2022.12.0.353 edn. Posit Software, PBC, Boston, MA
128. R Core Team (2022) R: A language and environment for statistical computing. 4.2.2 edn. R Foundation for Statistical Computing, Vienna, Austria
129. Serang S, Jacobucci R (2020) Exploratory mediation analysis of dichotomous outcomes via regularization. Multivariate Behav Res 55 (1):69-86. doi:10.1080/00273171.2019.1608145
130. Serang S, Jacobucci R, Brimhall KC, Grimm KJ (2017) Exploratory mediation analysis via regularization. Struct Equ Modeling 24 (5):733-744. doi:10.1080/10705511.2017.1311775
131. Babyak MA (2004) What you see may not be what you get: a brief, nontechnical introduction to overfitting in regression-type models. Psychosom Med 66 (3):411-421. doi:https://doi.org/10.1097/01.psy.0000127692.23278.a9
132. McNeish DM (2015) Using Lasso for Predictor Selection and to Assuage Overfitting: A Method Long Overlooked in Behavioral Sciences. Multivariate Behav Res 50 (5):471-484. doi:10.1080/00273171.2015.1036965
133. Tibshirani R (1996) Regression shrinkage and selection via the lasso. J R Statist Soc B 58 (1):267-288. doi:https://doi.org/10.1111/j.2517-6161.1996.tb02080.x
134. Tian Y, Zhang Y (2022) A comprehensive survey on regularization strategies in machine learning. Information Fusion 80:146-166. doi:10.1016/j.inffus.2021.11.005
135. Ammerman BA, Serang S, Jacobucci R, Burke TA, Alloy LB, McCloskey MS (2018) Exploratory analysis of mediators of the relationship between childhood maltreatment and suicidal behavior. J Adolesc 69:103-112. doi:10.1016/j.adolescence.2018.09.004
136. Hoerl AR, Kennard RW (2000) Ridge regression: Biased estimation for nonorthogonal problems. Technometrics 12 (1):80-86. doi:https://doi.org/10.2307/1271436
137. Zou H, Hastie T (2005) Regularization and variable selection via the elastic net. J R Stat Soc Series B Stat Methodol 67 (2):301-320. doi:https://www.jstor.org/stable/3647580
138. Jacobucci R, Grimm KJ, Brandmaier AM, Serang S, Kievit RA, Scharf F, Li X, Ye A (2022) regsem: Regularized structural equation modeling. 1.9.3 edn. doi:https://CRAN.R-project.org/package=regsem
139. Herlin B, Uszynski I, Chauvel M, Dupont S, Poupon C (2024) Sex-related variability of white matter tracts in the whole HCP cohort. Brain Struct Funct. doi:10.1007/s00429-024-02833-0
140. Bouhrara M, Rejimon AC, Cortina LE, Khattar N, Bergeron CM, Ferrucci L, Resnick SM, Spencer RG (2020) Adult brain aging investigated using BMC-mcDESPOT-based myelin water fraction imaging. Neurobiol Aging 85:131-139. doi:10.1016/j.neurobiolaging.2019.10.003
141. Buyanova IS, Arsalidou M (2021) Cerebral white matter myelination and relations to age, gender, and cognition: A selective review. Front Hum Neurosci 15:662031. doi:10.3389/fnhum.2021.662031
142. Kodiweera C, Alexander AL, Harezlak J, McAllister TW, Wu YC (2016) Age effects and sex differences in human brain white matter of young to middle-aged adults: A DTI, NODDI, and q-space study. Neuroimage 128:180-192. doi:10.1016/j.neuroimage.2015.12.033

bioRxiv preprint doi: https://doi.org/10.1101/2025.01.15.633108; this version posted January 15, 2025. The copyright holder for this preprint (which was not certified by peer review) is the author/funder. All rights reserved. No reuse allowed without permission.

143. Lawrence KE, Nabulsi L, Santhalingam V, Abaryan Z, Villalon-Reina JE, Nir TM, Ba Gari I, Zhu AH, Haddad E, Muir AM, Laltoo E, Jahanshad N, Thompson PM (2021) Age and sex effects on advanced white matter microstructure measures in 15,628 older adults: A UK biobank study. Brain Imaging Behav 15 (6):2813-2823. doi:10.1007/s11682-021-00548-y
144. Cox SR, Ritchie SJ, Tucker-Drob EM, Liewald DC, Hagenaars SP, Davies G, Wardlaw JM, Gale CR, Bastin ME, Deary IJ (2016) Ageing and brain white matter structure in 3,513 UK Biobank participants. Nature Communications 7 (1). doi:10.1038/ncomms13629
145. Price AL, Patterson NJ, Plenge RM, Weinblatt ME, Shadick NA, Reich D (2006) Principal components analysis corrects for stratification in genome-wide association studies. Nat Genet 38 (8):904-909. doi:10.1038/ng1847
146. Rosseel Y (2012) lavaan: An R package for structural equation modeling. J Stat Softw 48 (2):1-36. doi:10.18637/jss.v048.i02
147. Ocklenburg S, Güntürkün O (2018) Structural hemispheric asymmetries. In: The lateralized brain: The neuroscience and evolution of hemispheric asymmetries. Academic Press, London (United Kingdom), pp 239-262. doi:10.1016/b978-0-12-803452-1.00009-6
148. McDaniel M (2005) Big-brained people are smarter: A meta-analysis of the relationship between in vivo brain volume and intelligence. Intelligence 33 (4):337-346. doi:10.1016/j.intell.2004.11.005
149. Pietschnig J, Penke L, Wicherts JM, Zeiler M, Voracek M (2015) Meta-analysis of associations between human brain volume and intelligence differences: How strong are they and what do they mean? Neurosci Biobehav Rev 57:411-432. doi:10.1016/j.neubiorev.2015.09.017
150. Pakkenberg B, Gundersen HJ (1997) Neocortical neuron number in humans: effect of sex and age. J Comp Neurol 384 (2):312-320
151. Kevenaar JT, Hoogenraad CC (2015) The axonal cytoskeleton: from organization to function. Front Mol Neurosci 8:44. doi:10.3389/fnmol.2015.00044
152. Catani M, Thiebaut de Schotten M (2008) A diffusion tensor imaging tractography atlas for virtual in vivo dissections. Cortex 44 (8):1105-1132. doi:10.1016/j.cortex.2008.05.004
153. Benear SL, Ngo CT, Olson IR (2020) Dissecting the fornix in basic memory processes and neuropsychiatric disease: A review. Brain Connect 10 (7):331-354. doi:10.1089/brain.2020.0749
154. Raghavan S, Reid RI, Przybelski SA, Lesnick TG, Graff-Radford J, Schwarz CG, Knopman DS, Mielke MM, Machulda MM, Petersen RC, Jack CR, Vemuri P (2021) Diffusion models reveal white matter microstructural changes with ageing, pathology and cognition. Brain Communications 3 (2). doi:10.1093/braincomms/fcab106
155. Latini F, Trevisi G, Fahlstrom M, Jemstedt M, Alberius Munkhammar A, Zetterling M, Hesselager G, Ryttlefors M (2020) New insights into the anatomy, connectivity and clinical implications of the middle longitudinal fasciculus. Front Neuroanat 14:610324. doi:10.3389/fnana.2020.610324
156. Yin H, Zong F, Deng X, Zhang D, Zhang Y, Wang S, Wang Y, Zhao J (2023) The language-related cerebro-cerebellar pathway in humans: a diffusion imaging-based tractographic study. Quant Imaging Med Surg 13 (3):1399-1416. doi:10.21037/qims-22-303
157. Schmahmann JD, Guell X, Stoodley CJ, Halko MA (2019) The theory and neuroscience of cerebellar cognition. Annu Rev Neurosci 42:337-364. doi:10.1146/annurev-neuro-070918-050258
158. Jang SH, Lee SJ (2019) Corticoreticular tract in the human brain: A mini review. Front Neurol 10:1188. doi:10.3389/fneur.2019.01188
159. Akalu Y, Frazer AK, Howatson G, Pearce AJ, Siddique U, Rostami M, Tallent J, Kidgell DJ (2023) Identifying the role of the reticulospinal tract for strength and motor recovery: A scoping review of nonhuman and human studies. Physiol Rep 11 (14):e15765. doi:10.14814/phy2.15765
160. Wang Z, Wang J, Guo J, Dove A, Arfanakis K, Qi X, Bennett DA, Xu W (2023) Association of motor function with cognitive trajectories and structural brain differences: A community-based cohort study. Neurology 101 (17):e1718-e1728. doi:10.1212/WNL.0000000000207745

bioRxiv preprint doi: https://doi.org/10.1101/2025.01.15.633108; this version posted January 15, 2025. The copyright holder for this preprint (which was not certified by peer review) is the author/funder. All rights reserved. No reuse allowed without permission.

161. Chou MY, Nishita Y, Nakagawa T, Tange C, Tomida M, Shimokata H, Otsuka R, Chen LK, Arai H (2019) Role of gait speed and grip strength in predicting 10-year cognitive decline among community-dwelling older people. BMC Geriatr 19 (1):186. doi:10.1186/s12877-019-1199-7
162. James SN, Manning EN, Storey M, Nicholas JM, Coath W, Keuss SE, Cash DM, Lane CA, Parker T, Keshavan A, Buchanan SM, Wagen A, Harris M, Malone I, Lu K, Needham LP, Street R, Thomas D, Dickson J, Murray-Smith H, Wong A, Freiberger T, Crutch SJ, Fox NC, Richards M, Barkhof F, Sudre CH, Barnes J, Schott JM (2023) Neuroimaging, clinical and life course correlates of normal-appearing white matter integrity in 70-year-olds. Brain Commun 5 (5):fcad225. doi:10.1093/braincomms/fcad225
163. Koirala N, Perdue MV, Su X, Grigorenko EL, Landi N (2021) Neurite density and arborization is associated with reading skill and phonological processing in children. Neuroimage 241:118426. doi:10.1016/j.neuroimage.2021.118426
164. Sporns O, Tononi G, Edelman GM (2000) Connectivity and complexity: The relationship between neuroanatomy and brain dynamics. Neural Netw 13:909-922. doi:https://psycnet.apa.org/doi/10.1016/S0893-6080(00)00053-8
165. Riccomagno MM, Kolodkin AL (2015) Sculpting neural circuits by axon and dendrite pruning. Annu Rev Cell Dev Biol 31:779-805. doi:10.1146/annurev-cellbio-100913-013038
166. Haier RJ, Siegel BV, Nuechterlein KH, Hazlett E, Wu JC, Peak J, Browning HL, Buchsbaum MS (1988) Cortical glucose metabolic rate correlates of abstract reasoning and attention studied with positron emission tomography. Intelligence 12:199-217
167. Neubauer AC, Fink A (2009) Intelligence and neural efficiency. Neurosci Biobehav Rev 33 (7):1004-1023. doi:10.1016/j.neubiorev.2009.04.001
168. Jitsuishi T, Hirono S, Yamamoto T, Kitajo K, Iwadate Y, Yamaguchi A (2020) White matter dissection and structural connectivity of the human vertical occipital fasciculus to link vision-associated brain cortex. Sci Rep 10 (1):820. doi:10.1038/s41598-020-57837-7
169. Hua K, Zhang J, Wakana S, Jiang H, Li X, Reich DS, Calabresi PA, Pekar JJ, van Zijl PC, Mori S (2008) Tract probability maps in stereotaxic spaces: analyses of white matter anatomy and tract-specific quantification. NeuroImage 39 (1):336-347. doi:10.1016/j.neuroimage.2007.07.053
170. Mori S, Wakana S, van Zijl PCM, Nagae-Poetscher LM (2005) MRI atlas of human white matter. Elsevier B. V.,
171. Wakana S, Caprihan A, Panzenboeck MM, Fallon JH, Perry M, Gollub RL, Hua K, Zhang J, Jiang H, Dubey P, Blitz A, van Zijl PCM, Mori S (2007) Reproducibility of quantitative tractography methods applied to cerebral white matter. NeuroImage 36 (3):630-644. doi:https://dx.doi.org/10.1016%2Fj.neuroimage.2007.02.049
172. Miller EM (1994) Intelligence and brain myelination: A hypothesis. Pers Individ Differ 17 (6):803-832. doi:https://doi.org/10.1016/0191-8869(94)90049-3
173. Page D, Buchanan CR, Moodie JE, Harris MA, Taylor A, Valdes Hernandez M, Munoz Maniega S, Corley J, Bastin ME, Wardlaw JM, Russ TC, Deary IJ, Cox SR (2024) Examining the neurostructural architecture of intelligence: The Lothian Birth Cohort 1936 study. Cortex 178:269-286. doi:10.1016/j.cortex.2024.06.007
174. Abel S, Vavasour I, Lee LE, Johnson P, Ackermans N, Chan J, Dvorak A, Schabas A, Wiggermann V, Tam R, Kuan AJ, Morrow SA, Wilken J, Laule C, Rauscher A, Bhan V, Sayao AL, Devonshire V, Li DKB, Carruthers R, Traboulsee A, Kolind SH (2019) Myelin damage in normal appearing white matter contributes to impaired cognitive processing speed in multiple sclerosis. Journal of Neuroimaging 30 (2):205-211. doi:10.1111/jon.12679
175. Abel S, Vavasour I, Lee LE, Johnson P, Ristow S, Ackermans N, Chan J, Cross H, Laule C, Dvorak A, Schabas A, Hernandez-Torres E, Tam R, Kuan AJ, Morrow SA, Wilken J, Rauscher A, Bhan V, Sayao AL, Devonshire V, Li DKB, Carruthers R, Traboulsee A, Kolind SH (2020) Associations between findings from myelin water imaging and cognitive performance among individuals with multiple sclerosis. JAMA Netw Open 3 (9):e2014220. doi:10.1001/jamanetworkopen.2020.14220
176. Ouellette R, Mangeat G, Polyak I, Warntjes M, Forslin Y, Bergendal Å, Plattén M, Uppman M, Treaba CA, Cohen-Adad J, Piehl F, Kristoffersen Wiberg M, Fredrikson S,

bioRxiv preprint doi: https://doi.org/10.1101/2025.01.15.633108; this version posted January 15, 2025. The copyright holder for this preprint (which was not certified by peer review) is the author/funder. All rights reserved. No reuse allowed without permission.

Mainero C, Granberg T (2020) Validation of rapid magnetic resonance myelin imaging in multiple sclerosis. Annals of Neurology 87 (5):710-724. doi:10.1002/ana.25705
177. Khelfaoui H, Ibaceta-Gonzalez C, Angulo MC (2024) Functional myelin in cognition and neurodevelopmental disorders. Cell Mol Life Sci 81 (1):181. doi:10.1007/s00018-024-05222-2
178. Grasby KL, Jahanshad N, Painter JN, Colodro-Conde L, Bralten J, Hibar DP, Lind PA, Pizzagalli F, Ching CRK, McMahon MAB, Shatokhina N, Zsembik LCP, Thomopoulos SI, Zhu AH, Strike LT, Agartz I, Alhusaini S, Almeida MAA, Alnaes D, Amlien IK, Andersson M, Ard T, Armstrong NJ, Ashley-Koch A, Atkins JR, Bernard M, Brouwer RM, Buimer EEL, Bulow R, Burger C, Cannon DM, Chakravarty M, Chen Q, Cheung JW, Couvy-Duchesne B, Dale AM, Dalvie S, de Araujo TK, de Zubicaray GI, de Zwarte SMC, den Braber A, Doan NT, Dohm K, Ehrlich S, Engelbrecht HR, Erk S, Fan CC, Fedko IO, Foley SF, Ford JM, Fukunaga M, Garrett ME, Ge T, Giddaluru S, Goldman AL, Green MJ, Groenewold NA, Grotegerd D, Gurholt TP, Gutman BA, Hansell NK, Harris MA, Harrison MB, Haswell CC, Hauser M, Herms S, Heslenfeld DJ, Ho NF, Hoehn D, Hoffmann P, Holleran L, Hoogman M, Hottenga JJ, Ikeda M, Janowitz D, Jansen IE, Jia T, Jockwitz C, Kanai R, Karama S, Kasperaviciute D, Kaufmann T, Kelly S, Kikuchi M, Klein M, Knapp M, Knodt AR, Kramer B, Lam M, Lancaster TM, Lee PH, Lett TA, Lewis LB, Lopes-Cendes I, Luciano M, Macciardi F, Marquand AF, Mathias SR, Melzer TR, Milaneschi Y, Mirza-Schreiber N, Moreira JCV, Muhleisen TW, Muller-Myhsok B, Najt P, Nakahara S, Nho K, Olde Loohuis LM, Orfanos DP, Pearson JF, Pitcher TL, Putz B, Quide Y, Ragothaman A, Rashid FM, Reay WR, Redlich R, Reinbold CS, Repple J, Richard G, Riedel BC, Risacher SL, Rocha CS, Mota NR, Salminen L, Saremi A, Saykin AJ, Schlag F, Schmaal L, Schofield PR, Secolin R, Shapland CY, Shen L, Shin J, Shumskaya E, Sonderby IE, Sprooten E, Tansey KE, Teumer A, Thalamuthu A, Tordesillas-Gutierrez D, Turner JA, Uhlmann A, Vallerga CL, van der Meer D, van Donkelaar MMJ, van Eijk L, van Erp TGM, van Haren NEM, van Rooij D, van Tol MJ, Veldink JH, Verhoef E, Walton E, Wang M, Wang Y, Wardlaw JM, Wen W, Westlye LT, Whelan CD, Witt SH, Wittfeld K, Wolf C, Wolfers T, Wu JQ, Yasuda CL, Zaremba D, Zhang Z, Zwiers MP, Artiges E, Assareh AA, Ayesa-Arriola R, Belger A, Brandt CL, Brown GG, Cichon S, Curran JE, Davies GE, Degenhardt F, Dennis MF, Dietsche B, Djurovic S, Doherty CP, Espiritu R, Garijo D, Gil Y, Gowland PA, Green RC, Hausler AN, Heindel W, Ho BC, Hoffmann WU, Holsboer F, Homuth G, Hosten N, Jack CR, Jr., Jang M, Jansen A, Kimbrel NA, Kolskar K, Koops S, Krug A, Lim KO, Luykx JJ, Mathalon DH, Mather KA, Mattay VS, Matthews S, Mayoral Van Son J, McEwen SC, Melle I, Morris DW, Mueller BA, Nauck M, Nordvik JE, Nothen MM, O'Leary DS, Opel N, Martinot MP, Pike GB, Preda A, Quinlan EB, Rasser PE, Ratnakar V, Reppermund S, Steen VM, Tooney PA, Torres FR, Veltman DJ, Voyvodic JT, Whelan R, White T, Yamamori H, Adams HHH, Bis JC, Debette S, Decarli C, Fornage M, Gudnason V, Hofer E, Ikram MA, Launer L, Longstreth WT, Lopez OL, Mazoyer B, Mosley TH, Roshchupkin GV, Satizabal CL, Schmidt R, Seshadri S, Yang Q, Alzheimer's Disease Neuroimaging I, Consortium C, Consortium E, Consortium I, Consortium SYS, Parkinson's Progression Markers I, Alvim MKM, Ames D, Anderson TJ, Andreassen OA, Arias-Vasquez A, Bastin ME, Baune BT, Beckham JC, Blangero J, Boomsma DI, Brodaty H, Brunner HG, Buckner RL, Buitelaar JK, Bustillo JR, Cahn W, Cairns MJ, Calhoun V, Carr VJ, Caseras X, Caspers S, Cavalleri GL, Cendes F, Corvin A, Crespo-Facorro B, Dalrymple-Alford JC, Dannlowski U, de Geus EJC, Deary IJ, Delanty N, Depondt C, Desrivieres S, Donohoe G, Espeseth T, Fernandez G, Fisher SE, Flor H, Forstner AJ, Francks C, Franke B, Glahn DC, Gollub RL, Grabe HJ, Gruber O, Haberg AK, Hariri AR, Hartman CA, Hashimoto R, Heinz A, Henskens FA, Hillegers MHJ, Hoekstra PJ, Holmes AJ, Hong LE, Hopkins WD, Hulshoff Pol HE, Jernigan TL, Jonsson EG, Kahn RS, Kennedy MA, Kircher TTJ, Kochunov P, Kwok JBJ, Le Hellard S, Loughland CM, Martin NG, Martinot JL, McDonald C, McMahon KL, Meyer-Lindenberg A, Michie PT, Morey RA, Mowry B, Nyberg L, Oosterlaan J, Ophoff RA, Pantelis C, Paus T, Pausova Z, Penninx B, Polderman TJC, Posthuma D, Rietschel M, Roffman JL, Rowland LM, Sachdev PS, Samann PG, Schall U, Schumann G, Scott RJ, Sim K, Sisodiya SM, Smoller JW, Sommer IE, St Pourcain B, Stein DJ, Toga AW, Trollor JN, Van der Wee NJA, van 't Ent D, Volzke H, Walter H, Weber B, Weinberger DR, Wright MJ, Zhou J, Stein

bioRxiv preprint doi: https://doi.org/10.1101/2025.01.15.633108; this version posted January 15, 2025. The copyright holder for this preprint (which was not certified by peer review) is the author/funder. All rights reserved. No reuse allowed without permission.

JL, Thompson PM, Medland SE (2020) The genetic architecture of the human cerebral cortex. Science 367 (6484). doi:10.1126/science.aay6690
179. Schmitt JE, Raznahan A, Liu S, Neale MC (2020) The genetics of cortical myelination in young adults and its relationships to cerebral surface area, cortical thickness, and intelligence: A magnetic resonance imaging study of twins and families. Neuroimage 206:116319. doi:10.1016/j.neuroimage.2019.116319
180. Wu Y, Sun D, Wang Y, Wang Y, Ou S (2016) Segmentation of the cingulum bundle in the human brain: A new perspective based on DSI tractography and fiber dissection study. Front Neuroanat 10:84. doi:10.3389/fnana.2016.00084
181. Kemerdere R, de Champfleur NM, Deverdun J, Cochereau J, Moritz-Gasser S, Herbet G, Duffau H (2016) Role of the left frontal aslant tract in stuttering: a brain stimulation and tractographic study. J Neurol 263 (1):157-167. doi:10.1007/s00415-015-7949-3
182. Serrano-Sponton L, Lange F, Dauth A, Krenzlin H, Perez A, Januschek E, Schumann S, Jussen D, Czabanka M, Ringel F, Keric N, Gonzalez-Escamilla G (2024) Harnessing the frontal aslant tract's structure to assess its involvement in cognitive functions: new insights from 7-T diffusion imaging. Sci Rep 14 (1):17455. doi:10.1038/s41598-024-67013-w
183. Qian W, Khattar N, Cortina LE, Spencer RG, Bouhrara M (2020) Nonlinear associations of neurite density and myelin content with age revealed using multicomponent diffusion and relaxometry magnetic resonance imaging. Neuroimage 223:117369. doi:10.1016/j.neuroimage.2020.117369
184. Aboitiz F, Scheibel AB, Fisher RS, Zaidel E (1992) Fiber composition of the human corpus callosum. Brain Res 598:143-153. doi:https://doi.org/10.1016/0006-8993(92)90178-c
185. Liewald D, Miller R, Logothetis N, Wagner HJ, Schuz A (2014) Distribution of axon diameters in cortical white matter: an electron-microscopic study on three human brains and a macaque. Biol Cybern 108 (5):541-557. doi:10.1007/s00422-014-0626-2
186. Cao C, Zhang S, Wang J, Tian M, Ji X, Huang D, Yang S, Gu N (2024) PGS-Depot: a comprehensive resource for polygenic scores constructed by summary statistics based methods. Nucleic Acids Res 52 (D1):D963-D971. doi:10.1093/nar/gkad1029

bioRxiv preprint doi: https://doi.org/10.1101/2025.01.15.633108; this version posted January 15, 2025. The copyright holder for this preprint (which was not certified by peer review) is the author/funder. All rights reserved. No reuse allowed without permission.

Statements and Declarations

Acknowledgements

The authors would like to thank Wendy Johnson for providing the *g* factor scores, all research assistants for their support during the behavioral measurements, PHILIPS Germany (Burkhard Mädler) for the scientific support with the MRI measurements as well as Tobias Otto for technical assistance.

Funding

This work was supported by the Deutsche Forschungsgemeinschaft (GU 227/16-1).

Competing interests

The authors have no relevant financial or non-financial interests to disclose.

Author contribution

E.G., R.K., and O.G. conceived the project and supervised the experiments. E.G., C.St., R.K., and O.G. designed the project. R.K. and J.S.P. planned and performed genetic experiments. C.Sc. and C.F. collected data. C.St., E.G., J.S.P., D.M., and M.J.H. analyzed the data. C.St. and E.G. wrote the paper. All authors discussed the results and edited the manuscript.

Data availability statement

The data that support the findings of this study are available from the corresponding author upon reasonable request or can be downloaded from an Open Science Framework repository [https://osf.io/29cp6/]. We will release the data after our manuscript has been accepted for publication.

Ethics approval

The study was performed in line with the principles of the Declaration of Helsinki. Approval was granted by the Ethics Committee of the Faculty of Psychology at Ruhr University Bochum (vote Nr. 165).

Consent to participate

Informed consent was obtained from all individual participants included in the study.

Consent to publish

The authors affirm that human research participants provided informed consent for publication of the images in Figure 2.